Physics – Uspekhi **53** (9) 893 – 914 (2010)

REVIEWS OF TOPICAL PROBLEMS PACS numbers: **87.10. – e**, **87.15. – v**, **87.16. – b**

Molecular energy transducers of the living cell. Proton ATP synthase: a rotating molecular motor

Yu M Romanovsky, A N Tikhonov

DOI: 10.3367/UFNe.0180.201009b.0931

Contents

Abstract. The free energy released upon the enzymatic hydrolysis of adenosine triphosphate (ATP) is the main source of energy for the functioning of the living cell and all multicellular organisms. The overwhelming majority of ATP molecules are formed by proton ATP synthases, which are the smallest macromolecular electric motors in Nature. This paper reviews the modern concepts of the molecular structure and functioning of the proton ATP synthase, and real-time biophysical experiments on the rotation of the 'rotor' of this macromolecular motor. Some mathematical models describing the operation of this nanosized macromolecular machine are described.

> "If to describe the cell we were to choose between two extreme Models — a clock mechanism or a homogeneous gasphase chemical reaction — no doubt which of the two would have been chosen: the cell is much closer to a clock mechanism than to a purely statistical system."
>
> L A Blumenfeld [1]
>
> "ATP synthase is a splendid molecular machine... All enzymes are beautiful, but the ATP synthase is one of the most beautiful as well as one of the most unusual and important."
>
> P D Boyer [37]

1. Introduction

The notion of 'molecular machines' was coined 35 years ago (in the 1970s [1]) and is currently generally accepted in the scientific literature [1–27]. The molecular machine is a macromolecular structure, typically of natural origin (e.g., a protein molecule or complex), that converts chemical energy into the energy of directional motion of macromolecules or their fragments, transfers molecules and ions across biological membranes, and so on (see, e.g., recent reviews [7–16] and original articles [17–28]). The notion of enzymes as nanomolecular machines implies that they have a relatively small number of selected (mechanical) degrees of freedom associated with correlated motion of atomic groups or with the presence of mobile fragments [1–3, 29, 30]. This means that selected portions of a protein molecule or a protein complex can be regarded as macromolecular devices by analogy with elements of macroscopic machines and mechanisms.

From the physical standpoint, the main feature of *macromolecular machines and mechanisms* (MMMs) is a combination of *mechanical* and *statistical* properties [1–3, 29–32]. The mechanical properties of MMMs are determined by a large-scale structural rearrangement of macromolecules resulting from the motion of relatively large fragments of protein molecules along a small number of the selected degrees of freedom. The statistical properties of MMMs are due to thermal movements of individual atoms or their small groups. Thermal fluctuations of a macromolecular structure allow 'choosing' those microstates from the great number of them that cause chemical reactions to proceed as desired and ensure realization of the directed mechanical motion [2, 31–35].

The past decade has witnessed a revolution in the investigation of biological macromolecular machines; biophysicists have learned how to manipulate selected molecules of biopolymers using a magnetic or laser tweezer, measure physicochemical characteristics of individual macromolecules, and directly observe their movements (see [7–15]). X-ray structural analysis was used to elucidate the spatial structure of thousands of proteins; the architecture of various protein complexes was clarified. These approaches, taken

Yu M Romanovsky, A N Tikhonov Physics Department,
Lomonosov Moscow State University,
Vorob'evy gory, 119991 Moscow, Russian Federation
Tel. (7-495) 939 29 73
E-mail: yuromanovsky@yandex.ru, an_tikhonov@mail.ru,
an_tikhonov@physics.msu.ru

Received 26 March 2010, revised 23 April 2010
Uspekhi Fizicheskikh Nauk **180** (9) 931 – 956 (2010)
DOI: 10.3367/UFNr.0180.201009b.0931
Translated by Yu V Morozov; edited by A M Semikhatov

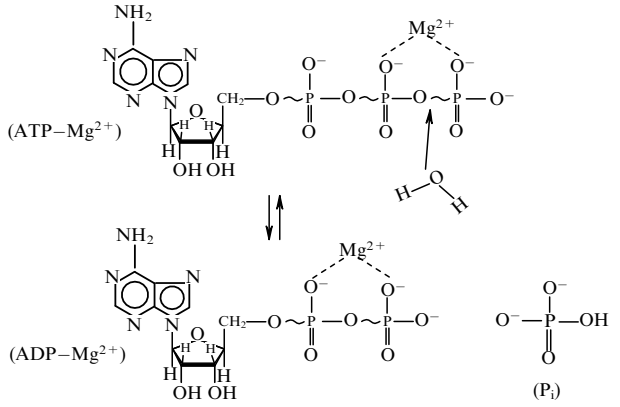

Figure 1. Structural formulas of adenosine triphosphosphate (ATP) and adenosine diphosphosphate (ADP).

together with modern biochemical and molecular biology methods for biopolymer research, have provided an insight into the mechanism of action of MMMs.

Studies of rotary MMMs are currently at the forefront of biophysical research. The molecular structure and physicochemical mechanisms of action of MMMs are widely discussed in the literature (see reviews [7–16]). Biological MMMs, whose work depends on the directional rotation of their rotor, are usually embedded in biological membranes and driven by the electrochemical potential difference generated across the membrane. Rotary MMMs contain ratchet-like elements that ensure directional motion of their rotor [31–35]. Presently, two families of natural nanosized rotary 'electric motors' are known. One comprises bacterial electric motors that drive flagellae of bacterial cells [32, 35]. A typical representative of the second family is F_0F_1 ATP synthase [36, 37], a protein complex responsible for the synthesis of adenosine triphosphoric acid or adenosine triphosphate (ATP), which is the main energy 'currency' of the living cell (Fig. 1). F_0F_1 ATP synthase is the smallest of the known natural electric motors [32, 37–45].

The work of a bacterial electric motor and F_0F_1 ATP synthase is based on similar principles, but the former is a much more complicated device than the latter. Bacterial electric motors have a stator embedded in the plasma membrane and a rotating rotor [32, 35]. The rotor is connected with a flagellum that is several orders of magnitude longer than the cell itself. The helical flagellum rotates as a 'propeller' and imparts translational movements to the cell. The transmembrane electric potential difference is the source of energy for rotor rotation in the bacterial flagellar motor. This complicated nanodevice has a molecular 'transmission gearbox' that permits changing the direction of rotation. Moreover, the bacterial cell has a molecular 'processor,' a macromolecular prototype of modern computers, that governs the behavior and spatial orientation of the cell. The 'processor' receives, stores, and analyzes information about the chemical composition and illumination of the environment coming from specialized receptors at the cell surface and emits specific signals to switch the direction of rotor rotation. This enables bacteria to change the direction of motion and move toward a target, i.e., an 'attractant' (nutritious substrate), or away from an ecologically unfavorable region containing so-called 'repellents.'

F_0F_1 ATP synthase is one of the most beautiful, unusual, and important molecular motors of the living cell. It occupies a special place among macromolecular energy transducers. F_0F_1-type ATP synthase protein complexes perform synthesis of the overwhelming majority of ATP molecules in the cell [46–49]. F_0F_1 ATP synthase, a unique energy transducer in the living cell, has *two rotary motors*. When synthesizing ATP, it works as a nanosized *electric motor* driven by the electrochemical potential difference of hydrogen ions ($\Delta\mu_{H^+}$) generated on the membrane in which this enzyme is embedded. The electric current running through the F_0 protein complex (the intramembranous fragment of F_0F_1 ATP synthase) drives the rotation of the rotor in the necessary direction; this, in turn, causes periodic conformational changes in the F_1 protein complex that directly catalyzes ATP synthesis. F_0F_1 ATP synthase not only synthesizes ATP molecules but also hydrolyzes them. In this case, the 'chemical energy' stored in ATP molecules is used to rotate the rotor inside the F_1 complex. The F_1 *mechanochemical motor* drives rotor rotation in the second motor, F_0, functioning as a 'proton pump' to generate $\Delta\mu_{H^+}$. The rotors of both motors, F_0 driven by the energy of $\Delta\mu_{H^+}$ and F_1 utilizing the ATP energy, are interconnected. There is direct experimental evidence that the two motors rotate during the work of F_0F_1 ATP synthase (see Section 4).

Today, the biochemical, mechanical, and kinematic properties of F_0F_1 ATP synthases of different origins are known fairly well. There is a substantial body of literature devoted to various aspects of the structural organization and mechanism of action of these unique macromolecular motors (see, e.g., reviews [31, 32, 36–45]. The aim of this article is to analyze the physicochemical mechanism of the F_0F_1 ATP synthase action and consider theoretical models describing this most important and unusual molecular machine of the living organism. The review is intended for a wide circle of readers, physicists, and biophysicists interested in macromolecular machines and nanobiomotors. It is organized into several levels differing in the degree of detail of the material in order to make it understandable and hopefully interesting to a wider audience. The article consists of 5 sections. Sections 1 and 2 contain general information necessary for understanding the physical mechanisms of the action of molecular motors. Sections 3 and 4 describe recent advances in the state of the art. Section 5 deals with mathematical simulation of rotary molecular motors.

2. ATP, the main energy 'currency' of the living cell

F_0F_1 ATP synthase complexes embedded in the membranes of mitochondria and chloroplasts (specialized energy-converting organelles of animal and plant cells, respectively), as well as bacteria, catalyze the synthesis of adenosine triphosphate (ATP) from adenosine diphosphate (ADP) and inorganic phosphate (P_i) (see Fig. 1). As mentioned above, the ATP molecule is the main energy 'currency' of the living cell. The overwhelming majority of energy-consuming biological processes, such as biosynthetic reactions, transmembrane transport of various molecules, and muscle contraction, involve the energy-donating reaction of ATP hydrolysis yielding ADP and inorganic phosphate (Fig. 2).

ATP hydrolysis ($ATP + H_2O \rightarrow ADP + P_i$) is accompanied by the release of energy that can be used for effective work. A decrease in the free energy of the system resulting from ATP hydrolysis in an aqueous solution under the so-called 'standard' conditions (concentration of reagents 1 M,

pH 7.0, temperature 25 °C) is $\Delta G^0_{ATP} = -7.3$ kcal mol^{-1} (30.5 kJ mol^{-1}) [47–50]. The 'standard' enthalpy of ATP hydrolysis characterizing the thermal effect of the reaction is $\Delta H^0_{ATP} = -5$ kcal mol^{-1} [50]. The energy released in ATP hydrolysis in an aqueous solution dissipates to heat. A major part of the energy resulting from ATP hydrolysis in biological systems is not wasted as heat, but is utilized for useful work (see Fig. 2).

The ATP hydrolysis and synthesis are reversible reactions ($ATP + H_2O \rightleftarrows ADP + P_i$). In the cell, they are catalyzed by enzymes (biocatalyzers) respectively known as ATPases and ATP synthases. ATPase ensures the work of muscular proteins, biosynthetic reactions, ion transfer across biological membranes, and other energy-consuming processes in the living cell due to the energy of ATP hydrolysis. The energy-donating hydrolytic reactions proceed parallel to ATP regeneration, compensating for the utilization of ATP in a variety of energy-consuming biochemical processes (see Fig. 2). The synthesis of ATP from ADP and P_i is catalyzed by ATP synthases using the energy from external sources (light in photosynthesing organisms, organic matter in bacteria and animals). F_0F_1-type ATP synthase complexes, to which this article is devoted, catalyze both reactions, ATP synthesis and ATP hydrolysis.

The ATP molecule is an ester of triphosphoric acid and adenosine, a derivative of adenine and ribose (see Fig. 1). Although the cleavage of the phosphoester bond in the ATP molecule releasing ADP and inorganic phosphate (P_i) is an energetically favorable process that can proceed without ATP hydrolyzing the enzymes, this reaction is very slow (for example, the ATP molecule preserves its structure in an aqueous solution for several months). The fact is that a relatively high energy barrier must be overcome in order for covalent bonds between phosphorus and oxygen to be broken in the ATP molecule. The reaction is substantially accelerated in the presence of enzyme catalyzing ATP hydrolysis. Characteristic turnover times of ATPases of different origins are $10^{-4}-10^{-2}$ s.

ATP synthesis is an energetically unfavorable process, largely because the phosphate groups of ADP and P_i molecules in aqueous solutions carry negative charges and a high energy barrier must be overcome to ensure their encounter necessary for the formation of a covalent phosphoester bond of the ATP molecule. Synthesis of the overwhelming majority of ATP molecules from ADP and P_i is catalyzed by specialized protein complexes (ATP synthases) embedded in energy-converting membranes. Conditions at catalytic sites of ATP synthases are favorable for ATP synthesis (see Section 3).

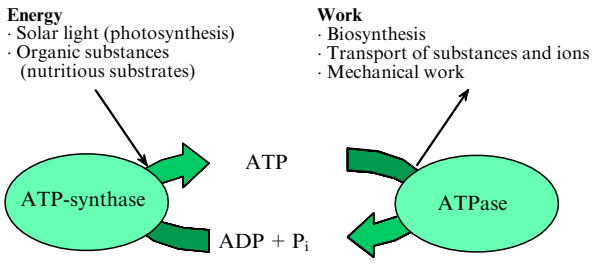

Figure 2. Schematic illustration of the leading role of the ATP molecule in coupling energy-donating and energy-accepting processes in the cell.

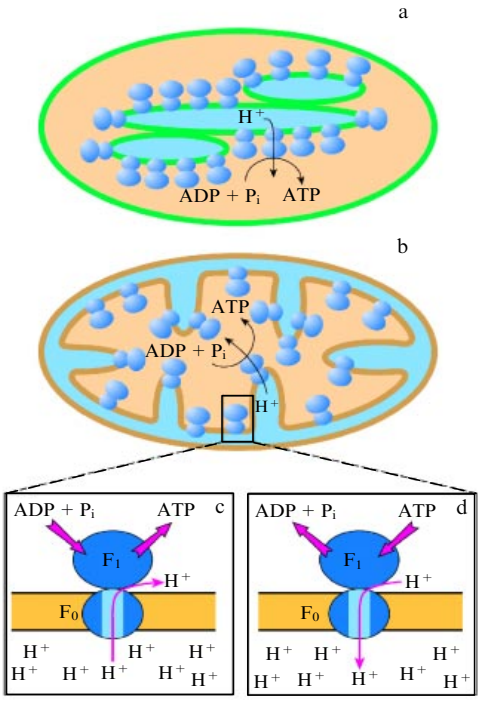

Figure 3. Schematic representation of the structure of chloroplast (a) and mitochondrion (b): energy-converting organelles of plant and animal cells. Dark shading shows regions of a high proton potential ('acidic pools'): the intrathylakoid compartment in chloroplasts and the space between inner and outer mitochondrial membranes. Light shading shows regions of a low proton potential ('alkaline pools'): the stromal space in chloroplasts and the so-called matrix space in mitochodria. Location of proton ATP synthase in the coupling membrane during ATP synthesis (c) and hydrolysis (d) are shown at the bottom.

The enzyme catalyzing ATP synthesis requires energy to be taken from an external source (see Fig. 2), such as solar light for photosynthesizing organisms, or free energy resulting from biological oxidation or organic compounds for animal and bacterial cells (see, e.g., Refs [46–49] for the details). In plants, ATP is produced in the photosynthetic electron transfer chain in chloroplasts (Fig. 3a). In animals, most ATP molecules form in mitochondria functioning as 'energy factories' (Fig. 3b) that use the energy released from oxidation (combustion) of organic matter (carbohydrates, fats, proteins) during so-called cellular respiration. This process is underlain by sequential oxidation of organic substances to CO_2 coupled with electron transfer to molecular oxygen (O_2) following a complex electron transport chain in mitochondrial membranes, which ends in the O_2 absorption (cellular respiration). Electron transport along the respiratory chain located in the inner membrane is coupled to transmembrane proton transfer, giving rise to a transmembrane electrochemical potential difference of hydrogen ions ($\Delta\mu_{H^+}$), which serves as a source of energy for ATP synthase. In chloroplasts, $\Delta\mu_{H^+}$ is generated on the membrane of thylakoids (closed vesicles in chloroplasts) (Fig. 3a) containing the photosynthetic electron transport chain. The function of this $\Delta\mu_{H^+}$-generating chain is maintained by solar energy.

The electrochemical potential difference of hydrogen ions ($\Delta\mu_{H^+}$) across the membrane (frequently referred to as the 'coupling' membrane) with the in-built ATP synthase complexes (Fig. 3c) is the 'proton-driving force' that initiates and

directs the work of ATP synthases. The value of $\Delta\mu_{H^+}$ is

$$\Delta\mu_{H^+} = F\Delta\varphi + RT \ln \frac{[H^+]_i}{[H^+]_o}, \quad (1)$$

where $\Delta\varphi = (\varphi_i - \varphi_o)$ is the transmembrane electric potential difference, $[H^+]_i$ and $[H^+]_o$ are hydrogen ion activities (concentrations) on two sides of the coupling membrane, R is the universal gas constant, T is the temperature [K], and F is the Faraday constant.

In energy-converting organelles of animal and plant cells (mitochondria, chloroplasts) and of bacterial cells, the 'proton potential' $\Delta\mu_{H^+}$ is 160–220 mV (11.6–19.3 kJ M^{-1}). The largest part of this energy is used to synthesize ATP from ADP and P_i.

As follows from formula (1), the value of $\Delta\mu_{H^+}$, frequently called the 'proton potential,' is the sum of two constituents, the electric ($\Delta\varphi = \varphi_i - \varphi_o$) and the concentration one, which originates from the difference between activities (concentrations) of hydrogen ions. The latter constituent is usually expressed in terms of the transmembrane pH difference, $\Delta pH = pH_o - pH_i = \lg([H^+]_i/[H^+]_o)$. The value of $\Delta\mu_{H^+}$ expressed in electrical units [V] at $T = 298$ K can be written as

$$\Delta\mu_{H^+} = \Delta\varphi + 0.06\,\Delta pH\ [V]. \quad (2)$$

As is known, both components (electric and concentration) compete as the driving force for ATP synthase [51]. A major contribution to $\Delta\mu_{H^+}$ in mitochondria is made by the electric potential difference $\Delta\varphi$ because the inner membrane containing ATP synthase complexes is a good dielectric. The mitochondrial membrane is poorly permeable to ions and therefore preserves the transmembrane electric potential difference $\Delta\varphi$ for a long time; moreover the pH difference is relatively small due to ion exchange processes, in the course of which protons transferred across the inner mitochondrial membrane bind to proteins and other molecules, forcing out other ions, e.g., K^+, into the intermembrane compartment. The transmembrane potential difference ($\Delta\varphi \approx 180-200$ mV) is maintained by virtue of the electroneutrality of ion exchange reactions (substitution of one positive ion by another) [46–48].

In plants, the situation is the opposite. The transmembrane electric potential difference $\Delta\varphi$ is bypassed due to the relatively high conductivity of thylakoid membranes for Mg^{2+}, K^+, Na^+, and Cl^- ions present in plant cells. As a result, the steady-state electric potential difference is usually small ($\Delta\varphi < 10-20$ mV), but the rather high transmembrane pH difference $\Delta pH \approx 1.5-2.5$ is maintained due to the permanent transmembrane proton flux created by the work of the electron transport chain [51–54].

3. Structural and functional organization of proton ATP synthases

The structure and main principles of the functioning of type-F_0F_1 proton ATP synthases have been elucidated in the last two to three decades. In 1997, British researcher John E Walker was awarded the Nobel Prize in chemistry for elucidation of the spatial structure of the F_1 protein complex, involved in that molecular machine. He shared his part of the prize with American biophysicist Paul D Boyer, who made a decisive contribution to the understanding of the mechanism of ATP synthesis. In what follows, we briefly consider structural and functional properties of ATP synthase.

3.1 The structure of proton ATP synthase

Figure 4 schematically presents the structure of F_0F_1-type ATP synthase embedded in an energy-converting membrane. The characteristic thickness of the membrane built up by lipid molecules (fat-like molecules constituting the main structural component of biological membranes) is 5 nm. A macromolecular complex of F_0F_1 ATP synthase consists of three morphologically distinct components: two relatively large protein complexes F_1 and F_0 (with F_1 exposed to the aqueous phase and F_0 embedded in the membrane) and a 'pedicle' connecting these complexes. In early ATP synthase studies, the protein complexes F_1 and F_0 were referred to as 'coupling factors' [46–49]. The intramembranous portion of this enzyme complex (F_0) is a hydrophobic (water-insoluble) protein. The other large fragment, the 'coupling factor' F_1, protrudes outside the membrane in the form of a spherical structure. In chloroplasts, F_0F_1 ATP synthase is embedded in thylakoid membranes (shown schematically as closed oblong vesicles in Fig. 3a), with the 'coupling factor' F_1 oriented toward the outer side, called stroma. In mitochondria, F_0F_1 ATP synthase is embedded in the inner membrane and the F_1 complex faces the matrix (the inner part of the mitochondrion).

The F_1 protein complex in plants and bacteria consists of nine protein subunits ($\alpha_3\beta_3\gamma\delta\varepsilon$) and has catalytic sites at which reactions of ATP synthesis and hydrolysis occur. The isolated, i.e., nonmembranous, F_1 complex is *adenosine triphosphatase* (ATPase) that catalyzes ATP *hydrolysis*. The 'coupling factor' F_0 embedded in the membrane (ab_2c_n protein complex) contains a proton-conducting channel; this complex ensures coupling between energy-donating processes of proton transport across the membrane and energy-accepting reactions of ATP synthesis that occur at the catalytic sites of F_1. The protein complexes F_1 and F_0 in bacteria, cyanobacteria, and chloroplasts of higher plants have a similar subunit composition, $\alpha_3\beta_3\gamma\delta\varepsilon$ and ab_2c_n, respectively. Mitochondrial F_0F_1 ATP synthase additionally contains several minor subunits [47, 48].

During ATP synthesis, the proton flux through ATP synthase is directed toward F_1 via F_0 (Fig. 3c). Protons are transferred via F_0 in the opposite direction during ATP hydrolysis (Fig. 3d). In this case, the enzyme functions as a

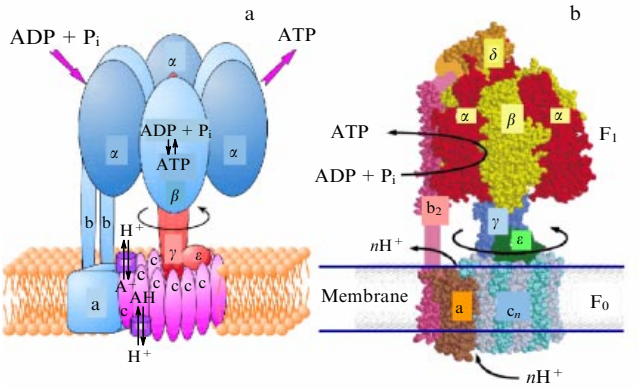

Figure 4. (a) Schematic representation of the structure of F_0F_1 ATP synthase. Light and dark shadingrespectively indicate protein subunits forming the 'stator' and the 'rotor.' Rotor rotation is associated with the transfer of hydrogen ions from the 'acidic' (bottom) to the 'alkaline' (top) pool. (b) Reconstruction of the 3D structure of F_0F_1 ATP synthase from the results of X-ray structural analysis [55, 56, 59].

proton pump (motor–generator) that produces $\Delta\mu_{H^+}$ by utilizing the ATP energy.

3.1.1 F_1 protein complex. The structure and spatial arrangement of the F_1 complex are well known. Details of the 3D structure of ATP synthases of various origins were elucidated by X-ray structural analysis. In 1994, Walker and co-workers were the first to report the atomic structure of the F_1 complex from bovine heart mitochondria (F_1 ATP synthase) at a 2.8 Å resolution [55]. Subsequently, plant and bacterial F_1 ATP synthases were described [56, 57].

Each of these F_1 ATP synthases is shaped as a globule ≈ 10 nm in diameter formed by three α-subunits and three β-subunits packed into an $\alpha_3\beta_3$ hexamer, an ensemble of six protein subunits. Homologous α- and β-subunits are polypeptide chains having a similar amino acid sequence and composition with minor differences. All the three β-subunits in the $\alpha_3\beta_3$ hexamers have a similar composition but different conformation. The same is true of α-subunits. The central cavity of $\alpha_3\beta_3$ contains an extended and slightly bent γ-subunit that protrudes outside from the globular $\alpha_3\beta_3$ hexamer (Fig. 4a). Figure 4b shows a model of the spatial structure of F_0F_1 ATP synthase reconstructed from the results of X-ray structural analysis [55]. Individual subunits of the enzyme are shaded differently.

The $\alpha_3\beta_3$ ensemble has the shape of a slightly flattened ball 8 nm in height and 10 nm in width. The ball has a hollow into which the γ-subunit is inserted, resembling a slightly bent shaft about 9 nm in length. Part of the γ-subunit protrudes from the $\alpha_3\beta_3$ hexamer 3 nm toward the intramembranous F_0 complex. This fragment of γ is linked to a relatively small ε subunit that regulates the enzyme activity. The mobile γ and ε subunits are components of the 'rotor' that rotates with respect to the 'stator' (the $\alpha_3\beta_3$ hexamer). The δ-subunit is located on the outer side of F_1 and plays an important structure-forming role; it is linked to b-subunits extending as projections from the intramembranous portion of the F_0 complex. The $\alpha_3\beta_3\gamma$ complex of seven subunits is the minimal structure capable of catalyzing ATP hydrolysis. The $\alpha_3\beta_3$ protein complex contains the catalytic sites of the enzyme at which ATP synthesis and hydrolysis occur.

3.1.2 F_0 protein complex. The hydrophobic (water-insoluble) protein complex F_0 embedded in the membrane makes up a base to which the F_1 complex is attached. It consists of a single a-subunit, two b-subunits, and several (9–14) identical replicas of a smaller c-subunit. The F_1 complex exposed to the aqueous phase is connected with the F_0 complex via two b-subunits that protrude from the membrane toward F_1. These subunits serve as fixed support structures linking F_1 and F_0. One α-helical segment of each b-subunit is embedded into the membrane, and the remaining part of the b-subunit protrudes from the membrane toward the F_1 complex and is attached to the δ-subunit on its surface (see Fig. 4). In addition, the F_1 and F_0 complexes are interconnected via the γ-subunit that extends from the $\alpha_3\beta_3$ hexamer to attach to the intramembranous ring c_n.

The c_n ring is formed by an ensemble of n c-subunits. Each c-subunit in the c_n complex is a relatively small protein in which two hydrophobic α-helices are connected via a short hydrophilic loop oriented toward F_1. In plants, the c_n ring consists of $n = 14$ c-subunits [58]; in yeast mitochondria, $n = 10$ [59]. The c_n ring is adjoined by a hydrophobic a-subunit also embedded into the membrane. Its polypeptide chain has six α-helical segments that traverse the membrane. The γ-subunit protrudes from the F_1 complex as far as the central part of the c_n 'ring.'

3.1.3 Proton-conducting pathway. The work of F_0F_1 ATP synthase depends on the directional rotation of its 'rotor' formed by the c_n ring connected to the γ- and ε-subunits (see Fig. 4). The rotor is driven by a torque created by the proton flux through F_0F_1 ATP synthase. In chloroplasts, the flux is directed outward, from the intrathylakoid space to the stroma; in mitochondria, the flux of hydrogen ions has the opposite direction, from the intramembranous space to the matrix. The proton channel through which hydrogen ions are transported from the region of a high proton potential ('acidic pool') to the region of a low proton potential ('alkaline or basic pool') is connected with the F_0 complex. Blockading this channel by inhibitors suppresses rotation of the rotor and ATP synthesis.

Protons transferred through F_0F_1 ATP synthase pass via F_0 along special 'channels' at the a–c-subunit interface. This pathway includes the following functionally important elements of the macromolecular construction (see Fig. 4):

(1) The c_n ring. The central part of each c-subunit contains a carboxyl group capable of binding a proton incoming from the acidic pool ($R-COO^- + H^+ \rightarrow R-COOH$) and releasing it into the alkaline pool ($R-COOH \rightarrow R-COO^- + H^+$).

(2) Two proton channels in the intramembranous part of F_0F_1 ATP synthase. One is located closer to the side of the membrane that faces the region with a high hydrogen ion concentration ('acidic pool'). This channel serves to deliver protons to the adjacent deprotonated group of the c-subunit ($R-COO^- + H^+ \rightarrow R-COOH$). Through the other channel exposed to the opposite side of the membrane, protons dissociate into the region with a low hydrogen ion concentration ('alkaline pool'). Being noncoaxial, the two channels are disconnected.

Amino acid residues of a- and c-subunits containing protonatable groups play a leading role in the work of the proton channels in F_0F_1 ATP synthase. These groups can retain and exchange protons. They are found in the residues of aspartate (Asp), arginine (Arg), histidine (His), and glutamate (Glu). The key role in proton transport through F_0F_1 ATP synthase of *E. coli* is played by the carboxyl group of aspartic acid in the c-subunit (Asp61, the number 61 indicating the position of the residue in the amino acid sequence counted from the N-terminus of the c-subunit polypeptide chain). Another important amino acid participating in proton transfer is arginine (Arg210) in the a-subunit. The guanidine group of Arg210 has a positive charge. The putative arrangement of these groups and the main stages of proton transfer via F_0 are shown in Fig. 5. Other amino acid residues of the a-subunit may also be involved in proton transfer through F_0F_1 ATP synthase, but their role in the creation of angular momentum is far less important than that of Asp61 and Arg210.

3.2 The mechanism of action of F_0F_1 ATP synthase

3.2.1 Catalytic sites of proton ATP synthase. Reactions of ATP synthesis and hydrolysis occur at catalytic sites of F_0F_1 ATP synthase located in the F_1 protein complex. When separated from the membrane, this complex no longer synthesizes ATP because it cannot use the energy of the transmembrane proton potential difference $\Delta\mu_{H^+}$. At the

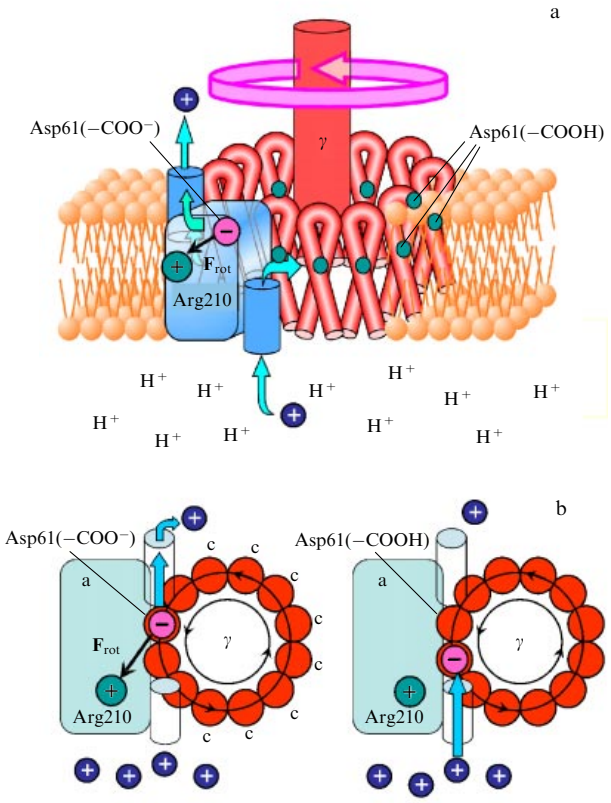

Figure 5. Schematic illustration of the transmembrane proton transfer via the intramembranous part of F_0F_1 ATP synthase and the mechanism of generation of a force $\mathbf{F}_{rot}$ creating the torque. (See the text for a detailed description of the proton-conducting pathway along which hydrogen ions are transferred from the 'acidic' to the 'alkaline' pool.)

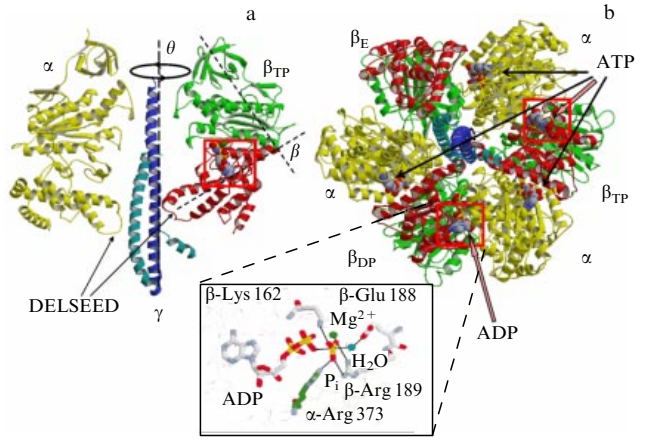

Figure 6. Spatial structure of the protein complex $\alpha_3\beta_3\gamma$. (a) Lateral view showing only three subunits, $\alpha\beta\gamma$; (b) top view. Thick arrows indicate ATP and ADP positions at the catalytic sites. Thin arrows show positions of three ATP molecules at noncatalytic binding sites. The inset below depicts ADP and F_1 molecules and their immediate vicinity inside the catalytic site of ATPase. (From the results of X-ray structural analysis of bovine heart mitochondrial F_1-ATPase [55].)

same time, the isolated complex containing even a minimal set of structural elements, $\alpha_3\beta_3\gamma$, continues to efficiently catalyze ATP hydrolysis; this reaction is energetically favorable and requires no energy from an external source.

The F_1 complex is known to have six binding sites for nucleotides (ATP or ADP) [36, 37]. Three of them are catalytic centers in which ATP synthesis and hydrolysis occur. Three others tightly binding nucleotides are not directly involved in these reactions. They are supposed to regulate the enzyme function [36, 37].

The catalytic sites are located in the clefts ('pockets') between neighboring α- and β-subunits of the $\alpha_3\beta_3$ hexamer (Fig. 6). Most functionally important groups of amino acids participating in the formation of catalytic sites belong to β-subunits. Site-directed mutagenesis experiments with selective substitution of amino acids demonstrated the key role of four residues in ATP synthesis and hydrolysis, three (β-Lys162, β-Arg189, and β-Glu188) on the β-subunit and one (α-Arg373) on the α-subunit (see Fig. 6; the nomenclature of amino acids corresponds to that of the bovine heart mitochondrial F_1-ATPase sequence [55]). These residues form a 'favorable' substrate (ADP and P_i) environment for ATP synthesis. The negative charges of the oxygen atoms in ADP and P_i are shielded by the positively charged groups of β-Lys162, β-Arg189, α-Arg373, and Mg^{2+} ion bound to ADP. As a result, the energy barrier for ATP synthesis from ADP and P_i decreases.

The three catalytic sites of F_1F_0 ATP synthase exhibit different affinities for ATP, ADP, and P_i. The difference can be accounted for as follows: all three α-subunits and three β-subunits making up the catalytic sites of the enzyme have a different conformation at each given instant due to conformational lability. X-ray studies of the structure of F_1-ATPase ($\alpha_3\beta_3\gamma$ complex) from bovine heart mitochondria [55] showed that one of the catalytic sites in the crystallized protein contains an ATP molecule (to be precise, its nonhydrlolyzable analog AMP–PNP). The oxygen atom between the second and the third phosphorus atoms in the AMP–PNP molecule is replaced by nitrogen, which prevents hydrolysis of AMP–PNP during crystallization. The second catalytic site is occupied by ADP and the third remains vacant. Evidently, the different affinities of these sites for nucleotides (ATP and ADP) is due to their structural differences.[1] The catalytic site containing tightly bound ATP has a 'closed' conformation (β_{TP}). The ADP-containing catalytic site is also closed, but its conformation β_{DP} is somewhat different from the β_{TP} conformation. The empty site has an 'open' β_E conformation. Penetration of substrates into the catalytic site β_E, unlike β_{TP} and β_{DP}, is sterically unrestricted. This structural feature of F_1-ATPase is equally characteristic of F_1-ATPases isolated from other organisms [57]. However, the β_{TP} and β_{DP} catalytic sites in some of the studied crystal structures composed of $\alpha_3\beta_3\gamma$ are filled in a different manner. According to Refs [60, 61], two catalytic sites contain ATP and the third remains vacant. It is supposed that these differences reflect different fixed conformational states of the enzyme depending on crystallization conditions.

Different properties of the β_E, β_{DP}, and β_{TP} catalytic sites are due to asymmetry of the $\alpha_3\beta_3\gamma$ complex. Probably, β- (and α-) subunits have different conformations because the $\alpha_3\beta_3$ hexamer contains an extended bent γ-subunit. Conformational variability is attributable to the flexibility of α- and

[1] Here and hereafter, it is implied (unless noted otherwise) that ATP and ADP molecules showing high affinity for Mg^{2+} ions form ATP–Mg^{2+} and ADP–Mg^{2+} complexes (see Fig. 1). Mg^{2+} ions are known to always participate in the processes proceeding in the catalytic centers of most known ATPases [36, 49].

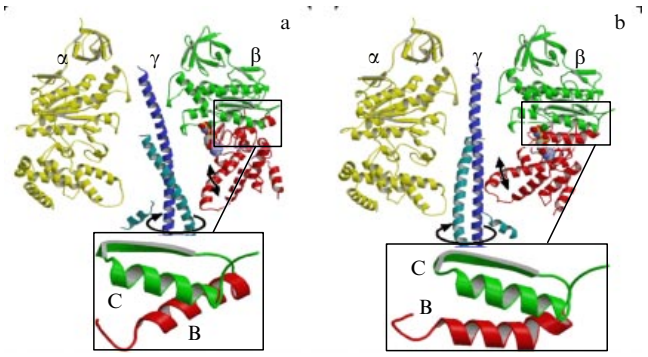

Figure 7. Position of the γ-subunit between the opposite α- and β-subunits: (a) 'open' conformation of a substrate-free catalytic site, (b) 'closed' conformation of a catalytic site containing $Mg^{2+}-ATP$. The data are based on the results of X-ray structural analysis of bovine heart mitochondrial F_1-ATPase [55]. Bottom insets show a change in the mutual arrangement of α-helical fragments B and C in the 'hinge' region of a β-subunit related to its structural rearrangement after binding an ATP molecule (Fig. 3 from [62] with modifications).

β-subunits, whose structure changes during rotation of the γ-subunit. Each *β*-subunit has two large domains (shown in Fig. 7 using dark and light shading) connected by a 'hinge.' The angle *β* characterizing the mutual arrangement of these domains changes by approximately 30° as the bent γ-subunit rotates (see Figs 7a and 7b). At the same time, the conformation of α-subunits changes less significantly.

The structural flexibility of the three β-subunits making contact with different sides of the bent γ-subunit thus enables them to acquire different conformations. Hence, the structural differences between the catalytic sites are manifested as their different affinities for ATP, ADP, and P_i. We emphasize that the bent γ-subunit is responsible for the asymmetry of the $\alpha_3\beta_3\gamma$ complex and, accordingly, for the different properties of the β_E, β_{DP}, and β_{TP} catalytic sites. Indeed, the X-ray structural analysis showed that an artificial $\alpha_3\beta_3$ complex without a γ-subunit is symmetric (with the C_3 symmetry) and all β- (and α-) subunits have a similar conformation [63].

An important structural feature of β-subunits is the characteristic loop extending toward the γ-subunit (see Figs 6 and 7). This fragment of the polypeptide chain, called DELSEED after its amino acid sequence, contains five negatively charged residues (D — aspartate, E — glutamate), one positively charged (L — lysine), and one neutral (S — serin). The fragment of the γ-subunit adjacent to DELSEED mostly contains positively charged residues. Interaction between the closely located charged fragments of β- and γ-subunits ensures mechanical coupling between these most important units of the macromolecular structure of F_1-ATPase. Due to the close contact between these fragments, a conformational change in a β-subunit induced by ATP binding to the catalytic site creates the torque that turns the rotor (rotation of the γ-subunit induced by ATP hydrolysis).

On the other hand, forced rotation of the γ-subunit connected to the rotor of the F_0 electric motor (which rotates using the energy of $\Delta\mu_{H^+}$) causes conformational changes to a β-subunit. They lead to a change in the state of catalytic sites of F_1 and synthesis of ATP from ADP and P_i. Drawing an analogy with macroscopic motors, it may be said that the eccentric γ-subunit rotated by the F_0 electric motor plays the role of a 'crankshaft'[2] that pushes β-subunits.

3.2.2 Catalytic cycles of ATP synthesis and hydrolysis. The work of F_0F_1 ATP synthase is accompanied by a structural rearrangement of the molecule, leading to synchronous changes in the state of all three catalytic sites. This section deals with the changes associated with rotor (γ-subunit) rotation inside the $\alpha_3\beta_3$ hexamer and their relation to ATP synthesis and hydrolysis reactions.

Unicentral catalysis. Mechanochemistry of ATP hydrolysis. We first consider the simplest scenario leading to ATP hydrolysis in a catalytic center of the enzyme. This scenario corresponds to the so-called unisite mechanism of catalysis realized at extremely low ATP concentrations (∼ 1 nM) when only one of the three sites contains an ATP molecule. Investigations of the unisite mechanism of catalysis have allowed evaluating energetics of the key stages of ATP hydrolysis [36, 64–68].

The sequence of these events can be written in a simplified form as

$$\mathrm{E} + \mathrm{ATP} \rightleftarrows \mathrm{E}_{\mathrm{ATP}} \rightleftarrows \tilde{\mathrm{E}}_{\langle \mathrm{ATP}\rangle} \underset{\text{ATP synthesis}}{\overset{\text{ATP hydrolysis}}{\rightleftarrows}} \tilde{\mathrm{E}}^{\langle \mathrm{P_i}\rangle}_{\langle \mathrm{ADP}\rangle} \rightleftarrows \mathrm{E}^{*}_{\langle \mathrm{ADP}\rangle} + \mathrm{P_i} \rightleftarrows \mathrm{E} + \mathrm{ADP} + \mathrm{P_i}\,, \quad (3)$$

where E denotes an empty catalytic site, E_{ATP} and $\tilde{E}_{\langle ATP\rangle}$ denote catalytic sites respectively containing a weakly and a tightly bound ATP molecule, $\tilde{E}^{\langle P_i\rangle}_{\langle ADP\rangle}$ is the catalytic site containing ADP and P_i, and $E^{*}_{\langle ADP\rangle}$ is the ADP-containing site.

The ATP hydrolysis and synthesis reactions are regarded as a sequence of individual reactions (3) proceeding in opposite directions.

We consider the energetics of the processes described by Eqn (3). The first act in the scenario leading to ATP hydrolysis is the binding of ATP to the enzyme. Its empty catalytic site exhibits high affinity for an ATP molecule. The binding is an energetically favorable process characterized under 'standard' conditions by a decrease in the free energy $\Delta G^0_{\langle ATP\rangle} \approx -(14-16)$ kcal mol^{-1} [64–68].[3] ATP binding occurs as a sequence of several elementary stages. The first is the diffusion of ATP from the solution into the open cleft between the adjacent α- and β-subunits housing the catalytic site. This process accelerates as the ATP concentration in the solution increases. ATP entry into the catalytic site induces a structural rearrangement of the protein, which results in the closure of the open catalytic site (Fig. 8). Structural analysis

[2] Animations illustrating conformational changes of ATP synthase and its subunits are freely available online at Walker's site (http://www.mrc-mbu.cam.ac.uk/research/atp-synthase/molecular-animations-atp-synthase). Some papers by G Oster and H Wang also contain references to various animations of this enzyme (see the references).

[3] We note that these ΔG^0 values characterize changes in the free energy under 'standard' conditions (the concentration of reagents 1 M, the temperature 25 °C, and pH = 7.0) in accordance with the formula $\Delta G^0 = -RT \ln K_{eq}$, where K_{eq} is the equilibrium constant of the reaction, R is the universal gas constant, and T is the temperature [K]. Because the free energy of ATP hydrolysis depends on the concentration of reagents as $\Delta G_{ATP} = \Delta G^0 + RT \ln\{([ADP]\cdot[P_i])/[ATP]\}$, the value of ΔG_{ATP} in real conditions may be significantly different from ΔG^0 [49].

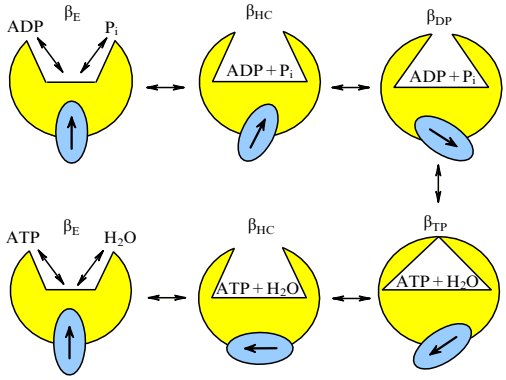

Figure 8. Schematic representation of the relations between chemical transformations of ADP, P_i, and ATP, structural changes in the β-subunit (transitions of the catalytic site from the 'open' to 'closed' state and back), and F_0F_1 ATP synthase rotor rotation. Symbols β_E, β_{DP}, and β_{TP} denote different conformational states of the catalytic site and β_{HC} denotes its 'half-closed' state.

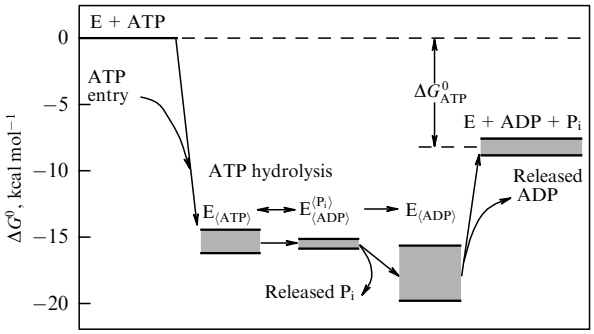

Figure 9. Diagram of free energy changes ΔG^0 during ATP hydrolysis by F_1-ATPase under 'standard' conditions (E is the enzyme molecule). The values of ΔG^0 are calculated as $\Delta G^0 = -RT \ln K_{eq}$. Equilibrium constants K_{eq} of individual reactions shown in the diagram are obtained from kinetic data for F_1-ATPases from bovine heart mitochondria [64, 65] and *E. coli* bacterium [66].

of F_1-ATPase and molecular dynamics calculations in [69] have allowed reconstructing the sequence of events related to the ATP binding. ATP penetration into the open cleft of the catalytic site is followed by the formation of 15–20 hydrogen bonds between ATP and amino acid residues of the catalytic site. ATP-induced conformational changes first affect the spatial structure of the β-subunit, where one domain rotates with respect to the other. As mentioned above, these changes are associated with a turn of the γ-subunit (see Section 3.2.1). They result in the closure of the formerly open catalytic site that holds the ATP molecule by hydrogen bonds. Their number increases to 15–20 as the catalytic site closes. Eventually, the ATP molecule is caught between two loops of the β-subunit and positively charged α-Arg373 of the α-subunit. Mg^{2+} plays an important role in the ATP transition from a weakly bound to a tightly bound state. Some authors [70] maintain that the energy of ATP binding partly (≈ 40%) transforms into the energy of elastic strain related to the bending of the β-subunit and deformation of its polypeptide chain segments forming the catalytic site. It is believed that the elastic strain energy of the β-subunit binding ATP is used for the work of other catalytic sites of F_1-ATPase [70].

Conditions inside a closed catalytic site favor rapid ATP hydrolysis. It was shown that multiple reversible interconversion of ATP and ADP ($ATP + H_2O \rightleftarrows ADP + P_i$) occurs in the closed site without energy consumption from an external source [36]. The equilibrium constant of this reaction is close to unity ($K_{eq} \approx 0.5-2.9$ [64–68]). This means that the free energy of the $ATP + H_2O \rightleftarrows ADP + P_i$ reaction at a closed catalytic site tends to zero: $\Delta G^0_{\langle ATP \rightleftarrows ADP+P_i \rangle} \approx 0$ kcal mol^{-1}. In other words, the ATP hydrolysis and synthesis reactions at the site do not require external energy. This confirms that the environment of ADP and P_i molecules at the catalytic site is favorable for the formation of covalent bonds between their phosphate groups.

The products of ATP hydrolysis dissociate into the solution. Evidently, this process is promoted by the repulsion of negative charges located near ADP and P_i molecules, which weakens the P_i binding to the catalytic site. As is known [64–68], dissociation of P_i is an energetically favorable process, with $\Delta G^0_{\langle P_i \rangle} \approx -(0.5-4)$ kcal mol^{-1}. The ADP molecule remaining after the P_i dissociation retains affinity for the catalytic site, and the 'standard' free energy of ADP dissociation is $\Delta G^0_{\langle ADP \rangle} \approx 7-12$ kcal mol^{-1}. The complete ATP hydrolysis cycle (Fig. 9) is an energetically favorable process ($\Delta G^0_{ATP \leftrightarrow ADP+P_i} \approx -(7-8)$ kcal mol^{-1}) that may occur spontaneously.

Realization of the process described by Eqn (3) leading to ATP synthesis is energetically unfavorable because it requires energy from an external source. Therefore, isolated F_1-ATPase is itself incapable of synthesizing ATP. However, under certain experimental conditions (see Section 4.1 below), even isolated F_1-ATPase may produce ATP using an external force that causes rotation of the γ-subunit. In what follows, we discuss at greater length how enzymatic catalysis accelerates ATP synthesis and hydrolysis reactions and which factors influence their rates.

Multicentral catalysis. Enzymes accelerate reactions that are very slow in their absence, e.g., spontaneous ATP hydrolysis. As mentioned above, the final stage in the sequence of reactions (3) leading to ATP hydrolysis is the energetically unfavorable ADP dissociation ($\Delta G^0_{\langle ADP \rangle} > 0$), which leads to a decrease in the overall hydrolysis rate. This probably explains why ATP hydrolysis by the unisite mechanism is five to six orders of magnitude slower than under real conditions, when a few catalytic sites are involved in the enzyme action (multisite catalysis [36, 37]). In this section, we show how the cooperation of several catalytic sites functioning in concert significantly (by 10^5-10^6 times) accelerates enzymatic reactions exemplified by ATP synthesis and hydrolysis. Due to such cooperation, realization of the energy-consuming stage (e.g., liberation of ADP from the catalytic site, $\Delta G^0_{\langle ADP \rangle} > 0$) is promoted by the energetically favorable process (ATP binding, $\Delta G^0_{\langle ATP \rangle} < 0$) in the other part of the enzyme. The catalytic centers in which *energy-donating* and *energy-accepting* processes occur are spatially separated but closely coupled via common elements of the macromolecular structure (in the case of F_0F_1 ATP synthase, it is the γ-subunit making contact with different subunits of the $\alpha_3\beta_3$ hexamer).

After preliminary remarks on the cooperation between catalytic sites, we consider the catalytic cycle of ATP synthesis at greater length. We note that high intracellular concentrations of ATP and ADP (∼ 1–10 mM) predetermine the multisite regime of enzyme action in which several (two or

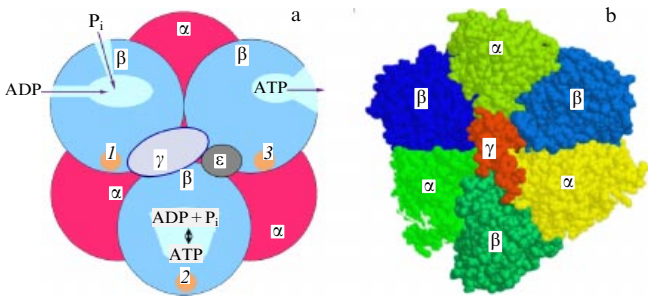

Figure 10. (a) Illustration of energy-dependent changes in the state of catalytic sites of F_0F_1 ATP synthase. (b) Mutual arrangement of α-, β-, and γ-subunits (see also Fig. 6) in F_1-ATPase deduced from the results of X-ray structural analysis [55].

three) nucleotides are simultaneously bound to different catalytic sites. Under these conditions, such sites involved in the ATP synthesis and hydrolysis function cooperatively. The central role in the coordination of the work of different catalytic sites is played by the rotating γ-subunit that ensures synchronous changes in the state of all three sites, which sequentially affect the affinity of each site for the substrates and products of the reaction.

We consider the ATP synthesis processes taking the cooperative interaction between all subunits of the enzyme into account. Figure 10 depicts three catalytic sites: *1* is the 'open' site accessible for the substrates (ADP and P_i), *2* is the 'closed' site with tightly bound ADP and P_i molecules capable of conversion into ATP, and *3* is the 'closed' site binding an ATP molecule. The vacant catalytic site (open site *1*) binds ADP and P_i. It closes under the effect of conformational changes in the enzyme caused by rotor rotation through 120° (transition from state *1* to state *2*). As a result, the ADP and P_i molecules find themselves in conditions favoring ATP synthesis without external energy. As noted above, the ATP production from ADP and P_i in the closed catalytic site requires no energy from an external source.

The next turn of the γ-subunit through 120° brings each of the three catalytic sites into a new state. The site in state *2* passes to state *3* in which it contains the ATP molecule produced from ADP and P_i without energy consumption. Importantly, this does not mean a violation of the energy conservation law. Indeed, the ATP molecule formed in this way remains tightly bound to the closed catalytic site and cannot be used for producing any effective work. The energy from an external source is needed to liberate this molecule and make it available for energy 'consumers.' Such a source is the electrochemical potential difference $\Delta\mu_{H^+}$ of hydrogen ions, which ensures rotation of the rotor of the F_0 electric motor. One more turn of the rotor through 120° again changes the state of the catalytic sites. Association of ATP with the enzyme weakens and it dissociates into the solution. Site *1* returns to its initial free state (transition from state *3* to state *1*).

We emphasize that the successive changes in conformational states of catalytic sites described above (see Fig.10, transitions $1 \rightarrow 2 \rightarrow 3$) result from the structural rearrangement of the enzyme initiated by rotor rotation using the energy from an external source ($\Delta\mu_{H^+}$). The cooperative character of such rearrangement accounts for its simultaneous effect on the state of all the three catalytic sites present in the $\alpha_3\beta_3$ hexamer. During the three successive turns of the rotor through 120°, i.e., its complete revolution, each catalytic site binds ADP and P_i molecules and releases one ATP molecule into the solution. Because ATP synthase has three catalytic sites, a new ATP molecule appears in the solution after each turn of the rotor by 120°.

This scenario corresponds to the so-called 'binding-change' mechanism proposed by Boyer [36, 37]. His hypothesis is based on two key postulates: (1) ATP synthesis from ADP and P_i in the active center of the enzyme does not require energy from an external source, (2) liberation of the tightly bound ATP molecule from a catalytic site is an energy-consuming process. Weakening of the ATP binding is due to the energy-dependent cooperative reorganization of the enzyme molecule (see the comprehensive review [36] for the history of the problem and different variants of the 'binding-change' mechanism). Experimental data on the structure of F_0F_1 ATP synthase are in good agreement with Boyer's mechanism of the action of this enzyme. Experimental evidence of the role of rotor rotation in the work of F_0F_1 ATP synthase is presented in Section 4.1.

As shown above, F_0F_1 ATP synthase is a reversible molecular machine, which means that the γ-subunit can rotate in the opposite direction in the presence of excess ATP molecules and in the absence of a proton potential. Under these conditions, the enzyme catalyzes ATP hydrolysis (ATP binding → ATP hydrolysis → dissociation of P_i and ADP). It is generally accepted that the ATP hydrolysis is the inverse of ATP synthesis (3). But concrete pathways of synthesis and hydrolysis do not necessarily coincide [2, 71] because the structural states of the enzyme catalyzing direct (ATP synthesis) and inverse (ATP hydrolysis) reactions may be significantly different. There are special biophysical and biochemical mechanisms regulating the activity of F_0F_1 ATP synthase by switching between its operation modes (catalysis of direct and inverse reactions; see [71] for the details). These mechanisms serve to optimize bioenergetic processes in the cell when its metabolic status (ATP/ADP ratio, and so on) changes. An important role in the switchover mechanism of F_0F_1 ATP synthase (ATP synthesis/hydrolysis) is played by the ε-subunit linked to the γ-subunit and located close to the c_n ring. A detailed analysis of this issue is beyond the scope of this review.

4. Proton ATP synthase: a rotating molecular motor

4.1 Experimental evidence of the rotor rotation

The available experimental data provide convincing evidence of the rotor rotation during the work of F_0F_1 ATP synthase. One group of experiments demonstrated the loss of enzyme activity when the rotor was fixed with respect to the stator. Experiments of the second group were designed to visualize rotor rotation by biophysical methods.

The first data that confirmed the rotor rotation in F_1-ATPase were obtained in experiments with chemical linking of the γ-subunit to one (radioactively labeled) of the three β-subunits based on the −S−S− bond formation between the adjacent cysteine residues of β- and γ-subunits [72–74]. It turned out that such artificial immobilization of the γ-subunit inhibited both hydrolysis and synthesis of ATP. The break of the linkage (−S−S− → −SH + HS−) restored enzymatic activity and the ability of ATP synthase to hydrolyze ATP. After the repaired enzyme worked for some time, the β- and

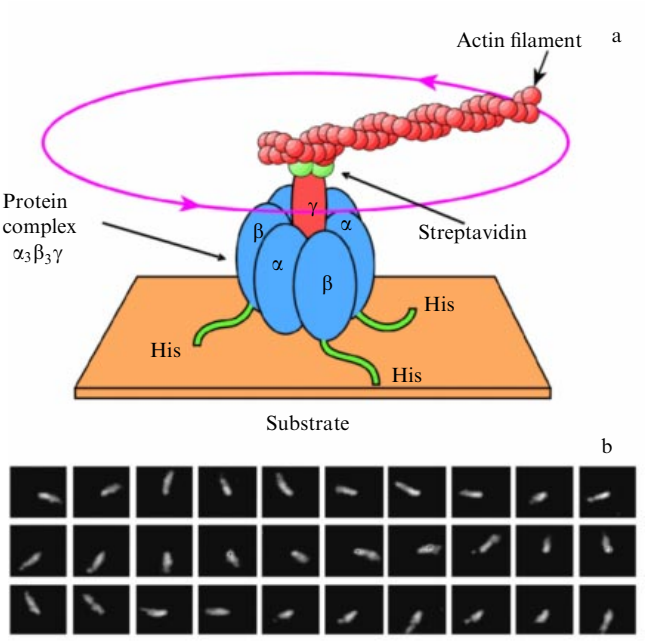

Figure 11. Schematic illustration of an experiment for visualization of rotor rotation in F_1-ATPase (based on [78, 142]); (a) construction of the hybrid system; (b) successive changes in the actin filament position (time intervals between images are 133 ms).

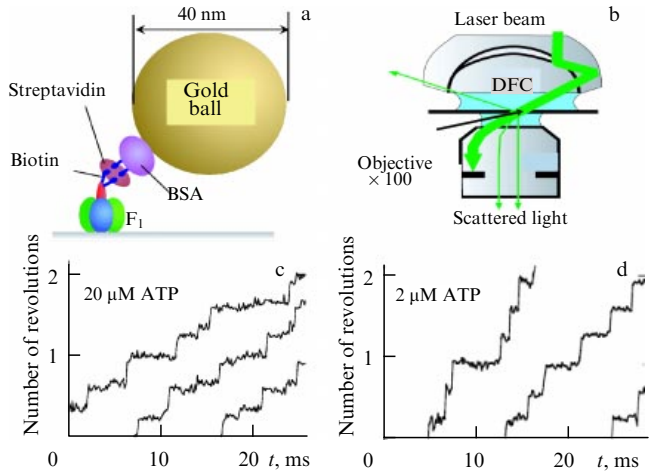

Figure 12. Illustrations of a rotor rotation experiment using the light scattering effect, based on [83]: (a) design of the hybrid system for observation of rotor rotation (BSA is bovine serum albumin); (b) schematic of the experimental setup (only scattered light enters the objective of the microscope, DFC is dark field condenser); (c, d) typical examples of bead rotation illustrating the discrete nature of rotor turns in a system containing 20 μM (c) or 2 mM (d) of ATP.

γ-subunits were linked again. The new links were not confined to the labeled subunit originally bound to the γ-subunit, but proved to be uniformly distributed between the three β-subunits. This finding suggested rotation of the γ-subunit in the presence of ATP.

Rotation of the γ-subunit during the work (ATP hydrolysis) of F_1-ATPase was demonstrated in [75–77] using fluorescent eosin covalently bound to the γ-subunit.

Direct observation of rotor rotation in an individual F_1-ATPase molecule was for the first time undertaken in 1997 by a group of Japanese researchers [78]. The macromolecular $\alpha_3\beta_3\gamma$ complex was attached to a hard substrate by artificial 'tails' fastened to β-subunits. Visualization of the γ-subunit rotation was made possible by the attachment of a macromolecular marker (∼ 1 μm long fluorescently labeled actin filament) to its end projecting from the $\alpha_3\beta_3$ hexamer (Fig. 11a). Microscopic observation of the fluorescent marker allowed elucidating the kinematics of the directional (counterclockwise) rotation of the γ-subunit with respect to the immobilized $\alpha_3\beta_3$ hexamer (Fig. 11b). It turned out that the directional rotation of the γ-subunit depended on the availability of the chemical 'fuel,' i.e., the ATP molecules. The direction of rotation was consistent with that predicted from the results of X-ray structural studies of the filling of catalytic sites by ATP and ADP molecules [78–80]. The rotation occurred in discrete steps of 120°. The mean rotor rotation rate increased to 10 rps with an increase in the ATP concentration in the solution surrounding the enzyme and a decrease in the marker length. Only occasional rare turns in either direction due to thermal fluctuations could be seen in the absence of ATP. Subsequent studies revealed the directional rotation of markers attached not only to the γ-subunit but also to other rotor elements, such as the c_n ring and ε-subunit [81]. Finally, the 'relativity' of the rotational motion initiated by the ATP hydrolysis was demonstrated. Experiments with the c_n ring immobilized on the substrate showed rotation of the marker attached to the $\alpha_3\beta_3$ complex [82].

In subsequent experiments (see, e.g., Ref. [83]), the marker was a gold bead 40 nm in diameter instead of the long (∼ 1 μm) actin tail (Fig. 12a). This permitted significantly decreasing the hydrodynamic resistance of the medium that slowed down the rotor rotation. The rotation of the bead tightly 'glued' to the γ-subunit with the protein streptavidin could be seen through a microscope (Fig. 12b). The measuring cell containing such a chimeric system placed under the microscope was illuminated by a laser beam. The experimental setup was designed such that only light scattered by the bead penetrated through the objective. Movements of the light spot served as indicators of bead rotation. This experiment allowed increasing the time resolution of the F_1-ATPase rotor rotation. Figures 12c, d are typical pictures of nanosize bead rotation during hydrolysis at different ATP concentrations [83]. At low concentrations (20 μM), each turn of the rotor through 120° is a two-phase event. A rapid turn by 80° – 90° (for ⩽ 0.25 ms) is followed by a 40° – 30° turn after a pause of ≈ 2 ms . The authors of [83] argue that phase 1 (80° – 90° turn) corresponds to the entry of ATP into a catalytic center and its hydrolysis there, and phase 2 (40° – 30° turn) corresponds to the dissociation of the reaction products (ADP and/or P_i).

The average bead rotation rate increases with the ATP concentration, probably because its waiting time at the empty catalytic site decreases. In this case, the two phases or rotor rotations can merge into one (Fig. 12d) because the next ATP molecule occupies the catalytic site almost immediately after it becomes vacant (40° – 30° phase) and initiates the turn by 80° – 90°.

The relation between the rotor rotation kinematics and chemical stages of ATP hydrolysis was thoroughly investigated in [84–89]. Figure 13 schematically illustrates changes in the properties of catalytic sites initiated by rotor rotation. The figure represents two possible scenarios demonstrating the relation between mechanical (rotor rotation) and chemical [ATP binding by the enzyme, ATP hydrolysis at a catalytic

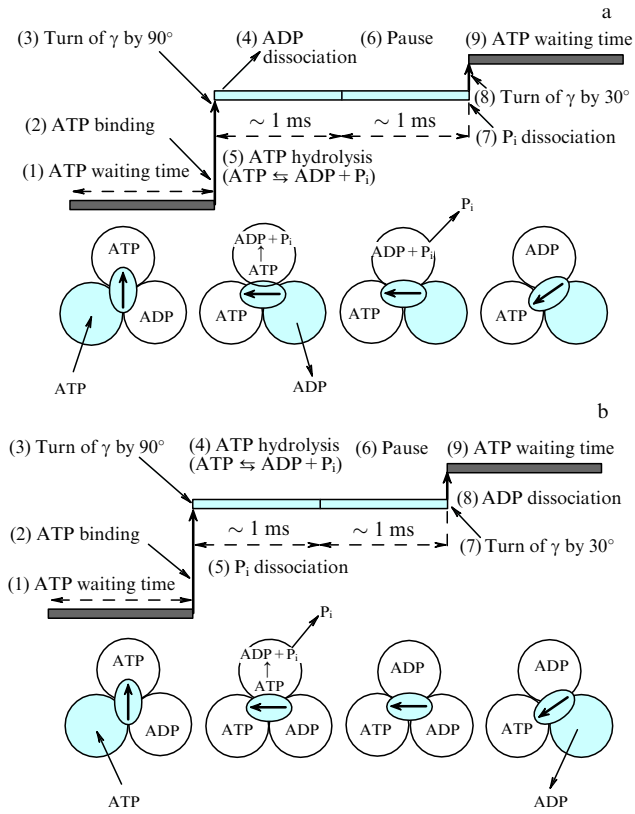

Figure 13. Schematic illustration of the relation between different phases of the catalytic ATP hydrolysis cycle and F_1-ATPase rotor rotation: (a) two-center mechanism; (b) three-center mechanism.

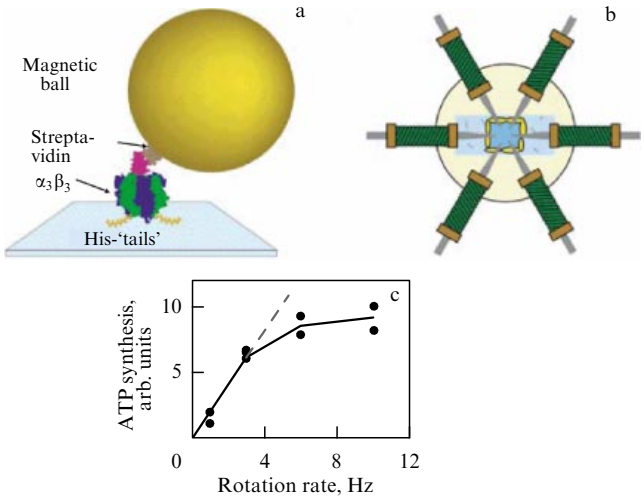

Figure 14. Schematic of the experiment on forced rotor rotation using a magnetic ball (Figs 1 and 4 from [95] with modifications): (1) general view of the motor (F_1 detail) with a magnetic bead attached; (b) top view of the experimental setup; (c) dependence of the ATP synthesis rate on the forced rotor rotation rate.

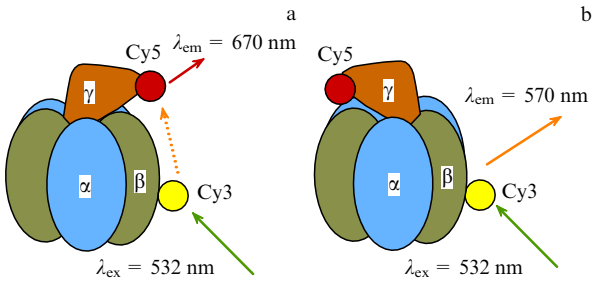

Figure 15. Schematic illustration of the possibility of recording rotor rotation of the molecular motor via the fluorescence resonance energy transfer between Cy3 and Cy5 dyes. The energy donor (Cy3) is attached to the stator (one of the three β-subunits of the F_1 molecule). The energy acceptor (Cy5) is attached to the rotor (γ-subunit). (Based on [96]). The donor and acceptor molecules come close together (a) or spread apart (b) as a result of rotor rotation.

site, dissociation of reaction products (ADP and P_i)] processes. These scenarios reflect bisite (Fig. 13a) and trisite (Fig. 13b) mechanisms of ATP hydrolysis (see Refs [36, 37, 90–94] for the details).

A beautiful work published in 2004 gave direct evidence that isolated F_1-ATPase containing even a minimal set of structural elements, $\alpha_3\beta_3\gamma$, functions as a *reversible molecular machine* [95]. It was shown that F_1-ATPase can function in one of the two regimes (ATP synthesis or hydrolysis), depending on the direction of forced rotor rotation. Rotation of the rotor in a desirable direction was achieved by attaching a magnetic 'handle' (magnetic bead, Fig. 14a) to the γ-subunit. F_1-ATPase molecules with magnetic 'handles' were fixed in a cell placed inside a system of controlled electromagnets rotating γ-subunits either clockwise or counterclockwise (Fig. 14b).

The results of the experiments were highly impressive. The clockwise rotor rotation (with the F_1-ATPase molecule viewed from the side of the γ-subunit projecting from $\alpha_3\beta_3$) promoted ATP synthesis from ADP and P_i, and the number of newly formed ATP molecules increased with an increase in the 'handle' rotation rate (Fig. 14c). Rotation of the 'handle' in the opposite direction was associated with ATP hydrolysis. The first-ever experimental evidence was thus obtained that isolated F_1-ATPase can function as a reversible molecular machine synthesizing or hydrolyzing ATP, depending on the direction of rotor rotation.

When F_0F_1 ATP synthase is embedded in a biological membrane, the direction of rotor rotation depends on which of the two motors creates the torque. Rotation of the rotor of a membranous electric motor (c_n ring) driven by the energy of the proton potential $\Delta\mu_{H^+}$ favors ATP synthesis. The hydrolysis regime (the excess of ATP and a low $\Delta\mu_{H^+}$ value) is maintained by the mechanochemical motor rotating the γ-subunit in the opposite direction, with the ATP energy being used to generate $\Delta\mu_{H^+}$. This mechanism is reminiscent of the work of a dynamo machine operating in two regimes, as an emf-generator driven by forced rotor rotation and as an electric motor rotating in the opposite direction when the induced emf is fed to the winding of the electromagnet. This allows regarding the F_0F_1 complex as a 'motor–generator.'

One more biophysical method for registration of rotor rotation in F_0F_1 ATP synthase is based on the fluorescence resonance energy transfer (FRET) [12, 96, 97], well known in optics and widely used in biophysics. In this method, two molecules of fluorescent dyes are inserted into the system of interest (the $\alpha_3\beta_3\gamma$ macromolecular complex) (Fig. 15). One molecule (Cy3) attached to the immobile β-subunit is excited by light of the wavelength 532 nm and emits light at $\lambda_{max} = 570$ nm. Another molecule (Cy5) is attached to the rotating γ-subunit and emits at $\lambda_{max} = 670$ nm. When the two dyes are sufficiently close, the Cy3 molecule excited by the

light of the wavelength 532 nm transmits excitation to Cy5, as can be seen from the Cy5 fluorescence at $\lambda_{max} = 670$ nm (Fig. 15a). As the distance between Cy5 and Cy3 increases under the effect of rotor rotation, the fluorescence at $\lambda_{max} = 670$ nm fades away and only Cy3 continues to emit at $\lambda_{max} = 570$ nm (Fig. 15b). This method is used in biophysics to register rotation of various macromolecular rotors [12].

The FRET technique was used to study rotor rotation in F_0F_1 ATP synthase. An advantage of this method is that rotor rotation is unhampered by relatively large markers (actin filaments or nanosized beads). Moreover, the work of F_0F_1 ATP synthase labeled by low-molecular-weight fluorescent dyes can be studied in model systems maximally consistent with the natural energy-converting intracellular apparatus. For example, fluorescence-labeled F_0F_1 ATP synthase molecules were built into liposomes (nanosize vesicles from membranes built up by lipid molecules) resembling chloroplast thylakoids. In such hybrid systems, the γ-subunit rotated in both ATP hydrolysis and ATP synthesis regimes. In the first case, the motor was driven by the energy of ATP molecules, and in the second case, by the rotation of the second motor, the c_n ring. The c_n ring of the intramembranous F_0 fragment was in turn rotated by the proton flux through F_0 when the pH difference (ΔpH) was artificially created across the liposome membrane [97]. It was thus proved that rotor rotation occurs in both the hydrolysis and synthesis of ATP when the energy source is ΔpH.

4.2 Torque generation mechanisms and motor efficiency

4.2.1 Mechanochemical motor of F_1-ATPase. Structural studies showed the presence of two regions of close contact between the rotor (γ-subunit) and the stator (see Figs 6a, 7) that serve as specific 'gates' allowing the substrate and reaction product access to the catalytic sites of F_1-ATPase. One contact region is situated in the central 'pocket' of the $\alpha_3\beta_3$ hexamer ('gate 1') into which the extended eccentric 'tail' of the γ-subunit is sunk. The other contact region is located outside, near the outer edge of the $\alpha_3\beta_3$ hexamer cavity, where the γ-subunit adjoins the DELSEED loop of the β-subunit ('gate 2'). According to Ref. [31], ATP reaches the empty catalytic site through 'gate 1' (G1 = γGln255). P_i formed during ATP hydrolysis in all probability leaves the catalytic site via 'gate 2' (G2 = γArg228). The torque arising at this site causes a turn of the γ-subunit in the course of conformational rearrangement of the adjacent β-subunit.

Indeed, experiments with F_1-ATPase mutants having γ-subunits with truncated 'tails' (preventing their contact with the stator in the depth of the cavity) showed that even in such defective molecules, the γ-subunit rotated in the right direction. This means that the torque is created mostly due to the interaction between the β- and γ-subunits at the periphery rather than in the depth of the cavity. Both structural data and results of calculations show [98] that the leading contribution to the angular momentum is made by electrostatic interactions of charged amino acid residues in the region of the contact between β- and γ-subunits. As mentioned above (Section 3.2.1), most amino acid residues in the DELSEED loop of the β-subunit adjacent to the γ-subunit carry a negative charge. The residues of the γ-subunit in contact with them are positively charged.

Although the lower portion of the γ-subunit 'tail' makes no significant contribution to the angular momentum, it seems to perform an important structural function. The region of contact between the β- and γ-subunits inside the cavity (G1) provides a 'foothold' for correct orientation of the γ-subunit with respect to the stator. Such mechanical 'adjustment' may be compromised in short rotors. Recent experiments in Refs [99–101] demonstrated that a truncated γ-subunit having no point of support undergoes irregular fluctuations during rotation, becoming slower compared with normal motors having extended γ-subunits. The low supporting point of long rotors prevents unwanted beats during rotation.

The experimental data in [80, 83] and the theoretical analysis of different operating modes of F_1-ATPase suggest that the γ-subunit rotation rate does not change during its turn [31, 32]. This means that the torque N also remains constant. The value of N was found from the dependence of the mean rotation rate of the F_1-ATPase rotor on the length of the actin filament attached to it. The torque created by ATP hydrolysis $N \approx 40-50$ pN nm [79, 80]. Bearing in mind that the rotor radius is about 1 nm, it is possible to calculate that the motor force is $F \approx 40-50$ pN. It is the largest force developed by the currently known natural molecular motors driven by the energy of nucleotide hydrolysis. As the rotor turns by 120°, the motor performs a work counter-hydrodynamic drag, $W \approx 80-90$ pN nm ($\approx 20k_BT$), roughly equal to a change in the free energy ΔG_{ATP} during hydrolysis of a single ATP molecule. These estimates indicate that the free energy of ATP hydrolysis is used to rotate a loaded rotor with the efficiency close to 100%.

Evidently, such a high efficiency of the F_1-ATPase motor ($\eta = W/\Delta G_{ATP}$) doing work against the forces exerted from the outside (hydrodynamic resistance of the medium slowing down the long 'tail' rotation) should be attributed to small energy losses due to friction during the γ-subunit rotation in the cavity of the $\alpha_3\beta_3$ hexamer. The low friction is due to design peculiarities of the motor. First, the extended γ-subunit has few direct contacts with the cavity walls. Second, the extended 'tail' of this subunit plunged into the cavity of the $\alpha_3\beta_3$ hexamer and the cavity itself have hydrophobic properties; they contain no electrostatically interacting charged groups that could hamper the rotor rotation. This property of the motor can be likened to the presence of a hydrophobic (oily) 'lubricant' layer between the rotor and the stator, which significantly decreases frictional losses.

4.2.2 Membranous electric motor F_0. A schematic illustration of proton transport through the intramembranous portion of F_0F_1 ATP synthase is presented in Fig. 5a. The two vertical cylinders symbolize proton-conducting channels. Along the lower channel, protons come from the 'acidic pool,' where their concentration is increased, to c-subunits. Along the upper channel, the protons are directed toward the 'alkaline pool,' where their concentration is low. The carboxyl group of Asp61 located in the central part of the c-subunit exists in two states, deprotonated ($-COO^-$) and protonated ($-COOH$). Its charge depends on the position relative to the upper or the lower proton-conducting channels. It undergoes protonation ($-COO^- + H^+ \rightarrow -COOH$) in the lower channel connected to the 'acidic pool' with the increased proton concentration. The carboxyl group of the neighboring c-subunit in the vicinity of the channel connected with the 'alkaline pool' is deprotonated, i.e., the proton dissociates and escapes to the

outside ($-COOH \rightarrow -COO^- + H^+$); as a result, the carboxyl group acquires a negative charge.[4]

Rotation of the c_n ring is maintained by the interaction of positively and negatively charged amino acid residues at the interface between the intramembranous a-subunit and one of the c-subunits of the oligomeric complex c_n. The key role in the creation of the torque is played by the positive charge of Arg210 of the intramembranous a-subunit and the negative charge of the deprotonated carboxyl group ($-COO^-$) of Asp61 (see Fig. 5). The distance between the atoms carrying these charges is roughly 2.5–3 Å [44]. Attraction between oppositely charged atoms creates the torque turning the ring through $\Delta\theta = 360^\circ/n$, where n is the number of c-subunits in the c_n complex (Fig. 5b, left side). After the turn, the deprotonated carboxyl group comes closer to the lower channel, acquires access to the 'acidic pool,' and becomes electroneutral ($-COO^- + H^+ \rightarrow -COOH$) (Fig. 5b, right side). After the next turn of the c_n ring, this protonated c-subunit departs from the a-subunit, taking with it the proton received from the 'acidic pool.' Moving counterclockwise together with the c_n ring, this protonated subunit comes to the upper channel after n rotation steps and releases the proton to the 'alkaline pool' to acquire a negative charge ($-COOH \rightarrow -COO^- + H^+$). Thus 'traveling' in a circular path, together with the rotating c_n ring, the proton is transferred from the 'acidic pool' to the 'alkaline pool.'

The source of energy for rotor rotation of the electric motor is the transmembrane electrochemical potential difference of hydrogen ions ($\Delta\mu_{H^+}$). The electric current running through F_0 (with protons as charge carriers) maintains periodic protonation/deprotonation of carboxyl groups in c-subunits and thereby creates conditions for directional rotor rotation. The c_n ring is tightly coupled to the γ-subunit functioning as the rotor of the F_1-ATPase mechanochemical motor. Due to this, the torque created by the F_0 motor is imparted to the γ-subunit, whose rotation governs the ATP synthesis.

4.2.3 Efficiency of the F_1-ATPase motor. A few remarks are in order regarding the estimates of motor efficiency cited in Section 4.1. The authors of experimental studies [79, 80] calculated the efficiency of the F_1-ATPase motor as follows. The kinematic data were used to determine the mean rotation rate $\langle\omega\rangle$ of the loaded rotor (heavy marker in a viscous medium). The drag coefficient ξ was found from geometric characteristics of the rotating 'tail' (cylindrical shaft of length L and radius r) by using the formula [80]

$$\xi = \frac{4\pi\eta L^3}{3\left[\ln(L/r) - 0.447\right]} . \qquad (4)$$

The average torque created by the motor is $\langle N\rangle = \xi\langle\omega\rangle$. The mechanical work against viscous drag forces during one revolution is $\xi\langle\omega\rangle 2\pi$. The chemical energy spent to produce this work is $3\Delta G_{ATP}$, where ΔG_{ATP} is the free energy of hydrolysis of a single ATP molecule that can be computed for the given experimental conditions (reactant concentrations, pH, and temperature).

The efficiency of utilization of the chemical energy of ATP molecules for the rotation of a loaded rotor is calculated as

$$\eta_{Stokes} = \frac{\overbrace{\xi\langle\omega\rangle\, 2\pi}^{\text{work}}}{\underbrace{3\Delta G_{ATP}}_{\text{free energy}}} . \qquad (5)$$

We note that the Stokes efficiency coefficient η_{Stokes} thus obtained is at variance with the traditional definition of the efficiency coefficient for machines working against conservative forces. In the present case, the work is done against a dissipative force, i.e., the force of hydrodynamic resistance of the aqueous medium. The estimates in Refs [79, 80] indicate that the work against internal friction forces is negligibly small compared with the work done for external load rotation. As mentioned above, the high efficiency of work against dissipative external forces ($\approx 90-100\%$) is attributable to the small internal energy losses due to design features of the F_1-ATPase motor.

Experimental data concerning the rotation of the γ-subunit with the attached long actin 'tail' depending on its length and the ATP concentration were analyzed theoretically in [31, 32]. It was shown there that the constancy of the angular momentum is an indispensable condition for the high efficiency of F_1-ATPase ($\eta_{Stokes} \approx 90-100\%$). Throughout the entire rotor rotation cycle, the motor must generate a constant torque ($N(\theta) \approx \text{const} = 40-45$ pN nm) rather than short, even if powerful, strokes at the instants of rapid turns. This means that the F_1-ATPase motor cannot operate based on the so-called Brownian ratchet mechanism when rotation is governed by rare powerful strokes reminiscent of a delta function (three short strokes per full revolution). According to [31, 32], the torque $N(\theta) \approx \text{const}$ can be generated as a result of many sequential stages, each accompanied by minor changes in the free energy ($\sim k_B T$). Such a gradual decrease in the free energy during the work of the F_1 mechanochemical motor may occur as many ($\sim 15-20$) hydrogen bonds between ATP and amino acid residues of the catalytic site form in succession [69].

5. Mathematical modeling of F_0F_1 ATP synthase

The MMMs have been studied theoretically by many foreign and Russian researchers (see Refs [31–34, 98, 102–116] and the references therein). Construction of mathematical models describing the directional motion of various nanomotors is an important area of research in theoretical biophysics. In this section, we briefly consider publications devoted to theoretical investigation of F_0F_1 ATP synthase. Biochemical and structural studies of F_0F_1 ATP synthase taken together with kinematic data on rotor rotation provided a wealth of experimental material for the development of a quantitative theory explaining the operating mode of this enzyme. The significance of such research is self-evident. Mathematical simulation is a convenient and sometimes the sole tool for the analysis of various scenarios underlying the work of MMMs and the assessment of their energetic and dynamic properties.

[4] We note that a change in the charge of the carboxyl group (protonation or deprotonation) occurs not only as a result of its contact with the 'acidic' or 'alkaline' pool but also due the difference in the electric potential on either side of the membrane. The affinity of the carboxyl group for protons increases with increasing the electric potential and decreases as it decreases. Therefore, a directional proton flux via F_0 occurs under the effect of the transmembrane electric potential difference, even in the absence of a transmembrane pH difference (a positive potential φ_i on the 'acidic pool' side and a negative potential φ_o on the 'alkaline pool' side). This accounts for the energetic equivalence of the electric ($\Delta\varphi$) and concentration (ΔpH) constituents of $\Delta\mu_{H^+}$ [51].

5.1 Dynamic models of operating proton ATP synthase

5.1.1 The simplest dynamic model of the F_0 rotor rotation. The first comprehensive models of rotor rotation in F_0F_1 ATP synthase were described in [102, 103]. They are discussed in Section 5.1.2 below. In this section, the analysis of rotor rotation begins from the consideration of the simplest dynamic model of rotor rotation in an electric motor (rotation of the intramembranous ring c_n) proposed in Refs [115, 116].

A qualitative description of the mechanism of generation of the angular momentum governing the directional rotation of the c_n rotor was presented in Section 4.2.2 (see Fig. 5). The dynamic equation describing rotor rotation in such a system and its solutions were considered in Refs [115, 116]. The simplified form of this equation is

$$I\,\frac{\mathrm{d}^2\theta(t)}{\mathrm{d}t^2}+4\pi\eta R^2h\,\frac{\mathrm{d}\theta(t)}{\mathrm{d}t}+M\bigl(\theta(t)\bigr)-\frac{R}{4\pi\varepsilon_0}\,\frac{|q_1q_2|}{\varepsilon r_1^2}\,\sin\bigl[\alpha\theta(t)+\varphi_0\bigr]=0\,, \tag{6}$$

where $\theta(t)$ is the rotation angle of the c_n ring, I is the moment of inertia of the intramembranous c_n ring, whose upper part is connected to the γ-subunit, R is the ring radius, h is the ring thickness, η is the cytoplasmic viscosity coefficient, $M(\theta(t))$ is the elastic force moment arising from the twist of the γ-subunit, q_1 and q_2 are the respective charges of Arg210 and Asp61, spaced r_1 apart, ε is the dielectric constant of the medium separating these charges, and α and φ_0 are coefficients depending on the system geometry and the number n of c-subunits.

The rotation of the c_n rotor proceeds stepwise. When the disk contains n c-subunits, a 120° turn of the rotor is associated with the passage of several protons through F_0 (their number must be at least $m=n/3$). The γ-subunit, having one end attached to the c_n ring and the other plunged inside the $\alpha_3\beta_3$ hexamer, is regarded as an elastic spring. The γ-subunit twists around itself after each turn of the ring by the angle $\Delta\theta=2\pi/n$. In earlier studies [117–119], it was assumed that the γ-subunit intertwines upon each turn of the c_n ring at the angle $2\pi/n$ and then at $2\pi/3$ (120°), and that the accumulated elastic strain energy is used for a structural rearrangement of the $\alpha_3\beta_3$ hexamer. For simplicity, we ignore other forces applied to the rotor. The moment created by the elastic tension force due to the rotor twist can be represented as

$$M\bigl(\theta(t)\bigr)=\frac{\pi R_\gamma^4E}{4h_\gamma(1+\sigma)}\,\bigl[\theta(t)+n\theta_\tau\bigr]\,, \tag{7}$$

where $R_\gamma=8$ Å is the radius and $h_\gamma=60$ Å is the length of γ-subunit, E is the Young modulus of the rotor, σ is the Poisson ratio (for most proteins, $\sigma=0.4$), and θ_τ is the twist angle of the γ-subunit during passage of a single proton. Then Eqn (6) takes the form

$$I\,\frac{\mathrm{d}^2\theta(t)}{\mathrm{d}t^2}+4\pi\eta R^2h\,\frac{\mathrm{d}\theta(t)}{\mathrm{d}t}+\frac{\pi R_\gamma^4E}{4h_\gamma(1+\sigma)}\bigl[\theta(t)+n\theta_\tau\bigr]-\frac{R}{4\pi\varepsilon_0}\,\frac{|q_1q_2|}{\varepsilon r_1^2}\,\sin\bigl[\alpha\theta(t)+\varphi_0\bigr]=0\,. \tag{8}$$

The solutions obtained describe the phenomenon under consideration correctly in general, but only at the qualitative level. The calculated torque ($N\sim4$ pN nm) is smaller by a factor of 10 than the experimentally found one, $N_{\mathrm{exp}}\approx40-50$ pN nm. Accordingly, the work done by the rotating disk is much smaller than the energy necessary for the synthesis of one ATP molecule. We note that the present model does not account for electrostatic interactions between charges and protons present in the 'inlet' and 'outlet' proton channels. The estimates of the dielectric constant ε in different layers of the model are questionable. Moreover, the model explicitly disregards the interaction between the γ-subunit and the $\alpha_3\beta_3$ hexamer. It is probably for this reason that the computed moments of 'resistance forces' are underestimated compared with experimental values, and the characteristic turn times are three orders of magnitude smaller than the real ones. Nevertheless, despite certain quantitative discrepancies, the above relatively simple model gives an idea of how the disk rotation mechanism operates. It is amenable to correction and can be improved based on the results of calculations described below (Section 5.1.2).

5.1.2 Description of rotor rotation in proton ATP synthase by stochastic dynamic methods. If a macromolecular motor has a relatively small moment of inertia of the rotor, the inertial term in the dynamic equation describing rotor rotation can be neglected compared to other terms. This allows writing the most general form of the equation for rotor rotation in the framework of the approach based on the stochastic Langevin equation [102, 103]:

$$\zeta\,\frac{\mathrm{d}\theta}{\mathrm{d}t}=F_{\mathrm{E}}(\theta,s)+F_{\mathrm{M}}(\theta,s)-\tau+f(t)\,, \tag{9}$$

where θ is the rotor rotation angle, ζ is the total drag coefficient, $F_{\mathrm{E}}(\theta,s)$ is the electrostatic force moment acting on the disk from the side of the a-subunit, $F_{\mathrm{M}}(\theta,s)$ is the 'hydrophobic' force moment acting on the disk from the side of the membrane, τ is the torque acting on the γ-subunit from the side of the $\alpha_3\beta_3$ hexamer, $f(t)$ is the moment of random impacts with the 'amplitude' $\sqrt{2\zeta k_{\mathrm{B}}T}$, and s characterizes discrete states of the system differing in the degree of filling of proton-binding sites of the F_0 motor. It is believed that the 'hydrophobic' force moment $F_{\mathrm{M}}(\theta,s)$ arises due to the energy barrier ($\sim45k_{\mathrm{B}}T$) preventing the displacement of charged (deprotonated) c-subunits toward the membrane. Four states of protonatable groups are taken into account: (a) the proton is bound to the carboxyl group of Asp61 in the c-subunit exposed to the 'acidic pool,' (b) the proton is bound to the carboxyl group of ASP61 in the c-subunit exposed to the 'alkaline pool,' (c) both carboxyl groups are protonated, and (d) both carboxyl groups are deprotonated. The model includes the interaction between negative charges of the deprotonated carboxyl groups of c-subunits moving together with the disk and the immobile positive charge of Arg210, as well as charges of other amino acid residues of the stator (Glu219, His245). Deformations of the γ-subunit caused by the c_n disk rotation were disregarded in [102]. It was assumed that the guanidine group of Arg210 is always charged positively ($q_{\mathrm{Arg210}}=+1$). The charge of the carboxyl group in the c-subunit may change; this group is characterized by $\mathrm{pK_a}=7.5$ ($\mathrm{pK_a}$ is equal to the pH value at which the acid group protonation probability is 50%).

The kinematics of rotor rotation is defined by the solution of Langevin equation (9) accounting for the Markovian process describing protonation and deprotonation of c-subunits in contact with proton channels. In the framework of

this model, a realistic description of the work of an electric motor was proposed in [102]. It was shown that the system can operate in two modes, as a generator of $\Delta\mu_{H^+}$ and as an electric motor driven by the energy $\Delta\mu_{H^+}$, and that rotor rotation is tightly coupled to the proton flux through the membrane. Indeed, one full revolution of the rotor is associated with the translocation of 12 protons, which corresponds to the transfer of 4 protons per synthesized ATP molecule. It is shown that the Arg210 residue plays a key role in the generation of angular momentum and in the maintenance of a close association between rotor rotation and the transmembrane proton transport. The presence of Arg210 prevents the proton leak, likely to occur for random reverse rotations of the rotor. The optimal operating regime of the electric motor is realized at $pK_a \approx 7$ for Asp61, in agreement with experimental data on the role of Asp61 in the generation of the angular momentum [120–123].

We note that a comprehensive rationale for the use of the Langevin equation for the description of the rotor rotation dynamics in a macromolecular electric motor was presented in Ref. [124] dealing with the work of the bacterial electric motor driving the flagellum of a bacterial cell. The design of such a motor is much more complicated than that of F_1F_0 ATP synthase. In the same work, a Markov chain of transitions characterizing rotor and stator conditions was constructed. The approach in Ref. [124] was used for the development of other nanomotor models.

The next study by Oster and Wang [103] concerned simulation of the F_1-ATPase mechanochemical motor accounting for changes in the state of catalytic sites $(\beta_1, \beta_2, \beta_3)$ in the $\alpha_3\beta_3$ hexamer and variations of the rotor (γ-subunit) loading. The system of equations describing F_1-ATPase rotor rotation has the form

$$\zeta \frac{d\theta}{dt} = \tau(\theta, \beta_1, \beta_2, \beta_3) - T_L + T_B(t), \tag{10}$$

$$\frac{d\beta_i}{dt} = K(\theta, \beta_{i-1}, \beta_{i+1})\,\beta_i, \tag{11}$$

where $i = 1, 2, 3$ labels the β-subunits, ζ is the drag coefficient due to rotor loading, $\tau(\theta, \beta_1, \beta_2, \beta_3)$ is the torque applied to the γ-subunit from the side of the $\alpha_3\beta_3$ hexamer, T_L is the additional moment created by the load (e.g., laser force clamp), $T_B(t)$ is the torque due to thermal fluctuations, the function $\tau(\theta, \beta_1, \beta_2, \beta_3) = -\partial V(\theta, \beta_1, \beta_2, \beta_3)/\partial\theta$ is determined by a potential $V(\theta, \beta_1, \beta_2, \beta_3)$ in which geometric and elastic properties of the system are taken into account, and $K(\theta, \beta_{i-1}, \beta_{i+1})$ is the matrix describing transition rates between the 64 possible states of catalytic sites depending on the rotation angle of the γ-subunit and the 'chemical' state of the system.

It is assumed that ATP hydrolysis and synthesis reactions are reversible and each catalytic site E can be in four possible states: (1) E is a free site, (2) E_T is occupied by an ATP molecule, (3) E_D is occupied by an ADP molecule, and (4) E_{DP} is occupied by ADP and P_i molecules. The enzyme has three catalytic sites; therefore, the maximum number of its states is $4^3 = 64$ (four possible states of three catalytic sites).

Solving the system of equations (10), (11) has allowed quantitatively describing the main features of the F_1-ATPase rotor rotation: step-by-step turns by $2\pi/3$, generation of the torque $N \approx 45$ N nm, consumption of one ATP molecule per a $2\pi/3$ turn, and the efficiency close to 100%. The results of calculations are in excellent agreement with the idea that the ATP binding energy is stored in the form of the elastic strain energy used to rotate the γ-subunit due to the tight coupling between the mechanical and chemical stages of the F_1-ATPase operation (see Section 5.4 for the details).

The model of F_1-ATPase operation described in Ref. [103] belongs to a class of mathematical models called 'mesoscopic models' or Markov–Fokker–Planck (MFP) models. Models of this type are intermediate between molecular dynamic ones (describing the motion of each atom) and kinetic models describing transitions between a relatively small number of discrete chemical ('Markovian') states. A very important step in the construction of MFP models is the choice of a small number of distinguished degrees of freedom considered in the explicit form and the construction of free energy surfaces for which these degrees of freedom are geometric coordinates. Such surfaces are usually constructed based on structural (X-ray structural analysis) and biochemical data that permit identifying the most important interactions between different subunits.

A classic example of MFP models used to describe F_0F_1 ATPase is the model proposed in [126]. The authors assumed that the reactions of ATP hydrolysis and synthesis proceeding as in (3) are reversible and that each catalytic site E is in four possible states: E, E_T, E_D, or E_{DP}. The probability ρ_s of being in each of these states can be described by the Kolmogorov–Fokker–Planck equation

$$\frac{\partial\rho_s}{\partial t} = -\frac{D}{k_B T}\frac{\partial}{\partial\theta}\left(-\frac{\partial\hat{G}(\theta, s)}{\partial\theta} + \tau\right)\rho_s + D\frac{\partial^2\rho_s}{\partial\theta^2} + \sum_{s'} K_{ss'} \times \rho_{s'}, \tag{12}$$

where $D = 1.5 \times 10^4$ rad^2 s^{-1} is the diffusion coefficient for rotor rotation of the F_1 mechanochemical motor (γ-subunit) and τ is the torque created by the rotor of the F_0 electric motor. For simplicity, it is assumed that $\tau = \text{const} = 45$ pN nm. The torque acting on the γ-subunit from the side of β-subunits is determined by the $\gamma-\beta$ interaction potential, $-\partial\hat{G}(\theta, s)/\partial\theta$. The potential $\hat{G}(\theta, s)$ is the sum of potentials of the γ-subunit interaction with three different β-subunits:

$$\hat{G}(\theta, s) = G(\theta)_{s_1} + G\left(\theta + \frac{2\pi}{3}\right)_{s_2} + G\left(\theta + \frac{2\pi}{3}\right)_{s_3}. \tag{13}$$

The form of $\hat{G}(\theta, s)$ is described in Ref. [126], where the values of the $K_{ss'}$ matrix elements characterizing the kinetics of transitions from one state to another are also given. The appendix to [126] presents an animated picture illustrating the work of the system.

The results in Ref. [126] indicate that at the 'mesoscopic' level' (millisecond time scale, nanosized system), the model adequately describes the mechanochemical properties of the F_0F_1 complex synthesizing ATP. The rotation angle θ of the γ-subunit can be used as a generalized ('collective') coordinate, a surrogate multidimensional periodic trajectory of the coordinates of the atoms making up the catalytic sites. The results of stationary solutions of Eqns (12), (13), and $\partial\rho_s/\partial t = 0$, related to F_0F_1 ATPase operation during ATP synthesis, are in excellent agreement with experiment [126]. Another interesting result of simulation of the F_0F_1 ATP synthase is that there are many trajectories (rather than one) of transition between different enzyme states under real physiological condition. The results of such a simulation

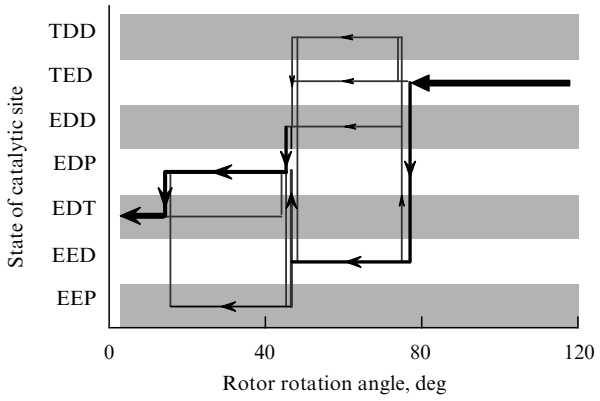

Figure 16. Schematic illustration of different pathways of F_1-ATPase evolution during rotation of its rotor. The letters T, D, and E denote three possible states of the catalytic sites: T — the site contains ATP, D — the site contains ADP, E — the site is vacant. The thickness of each line designating transition is proportional to its statistical weight (based on [128]).

allow estimating the statistical weight of these trajectories and identifying the so-called 'main kinetic pathway' (Fig. 16). Also, the model permits clarifying the well-known phenomenon of F_1-ATPase inhibition by ADP, which has long remained unexplained by biochemists [36].

5.2 Electrostatic interactions and energetics of ATP hydrolysis

Conformational changes in F_1-ATPase induced by ATP binding to a catalytic site, as well as by ATP hydrolysis and dissociation of reaction products, are accompanied by a redistribution of electric charges in the protein molecule. It is therefore important to estimate the contribution of electrostatic interactions to the energetics of ATP hydrolysis [111–114]. A simple way to calculate the energy of electrostatic interactions of charged groups of F_1-ATPase and all reactants bound to the enzyme was described in our work [127, 129].

The energy of electrostatic interactions $E_{\rm el}$ was assessed using the approximation of point-like charges at the geometric centers of the respective atoms. The energy $E_{\rm el}$ of the enzyme–substrate complex was estimated from the formula

$$E_{\rm el} = \frac{1}{2}\sum_{i=1}^{M}\sum_{\substack{j=1\\(j\neq i)}}^{M}\frac{Q_iQ_j}{\varepsilon_{\rm eff}|\mathbf{R}_i-\mathbf{R}_j|} + \sum_{i=1}^{M}\sum_{k=1}^{N}\frac{Q_iq_k}{\varepsilon_{\rm eff}|\mathbf{R}_i-\mathbf{r}_k|} + \frac{1}{2}\sum_{k=1}^{N}\sum_{\substack{m=1\\(k\neq m)}}^{N}\frac{q_kq_m}{\varepsilon_{\rm eff}|\mathbf{r}_k-\mathbf{r}_m|}, \qquad (14)$$

where Q_i is the electric charge of the ith atom in the substrate or a product molecule located at the catalytic center, q_k is the electric charge of the kth atom in the protein molecule, M is the number of charged substrate atoms (ATP^{4-}, ADP^{3-}, HPO_4^{2-}, and Mg^{2+}), $\mathbf{R}_i$ $(i=1,\ldots,M)$ and $\mathbf{r}_k$ $(k=1,\ldots,N)$ are respectively the coordinates of the substrate and enzyme atoms, and $\varepsilon_{\rm eff}$ is the effective dielectric permittivity (a model parameter).

In Ref. [127], we took the charges of lysine, arginine, aspartate, glutamate, and histidine residues into account. It was assumed that the point-like charge of lysine $q_{\rm Lys}=+1$ is

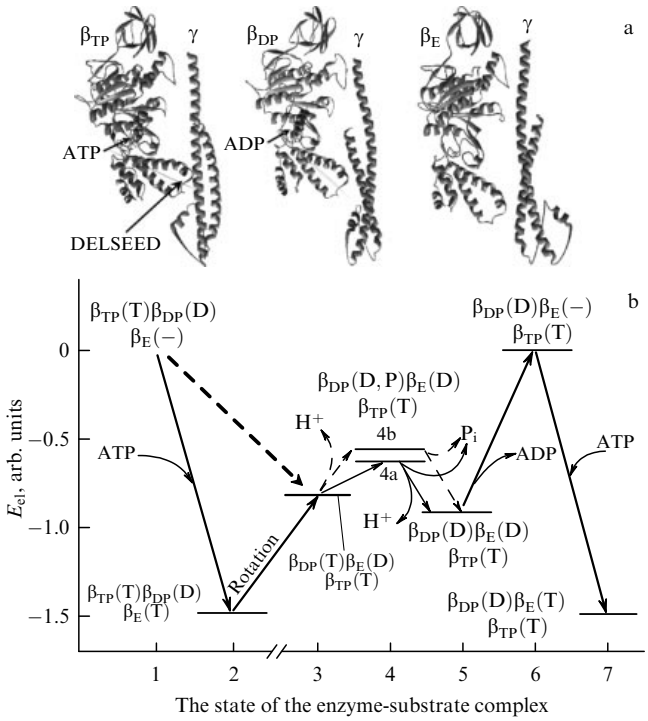

Figure 17. (a) Three possible conformations of a β-subunit corresponding to catalytic sites β_{TP}, β_{DP}, and β_E. (b) Diagrammatic representation of changes in the electrostatic constituent of energy ($E_{\rm el}$) for different states of F_1-ATPase catalytic sites [127].

associated with the nitrogen atom of the amino group. For arginine, the point-like charges $q_{\rm Arg}=+0.5$ at the two terminal nitrogen atoms were considered. In histidine, the charges $q_{\rm His}=+0.5$ were assigned to the two nitrogen atoms of the imidazole ring. In carboxyl groups of glutamate and aspartate, the similar partial charges $q=-0.5$ were distributed between the two oxygen atoms.

Conformational changes of all subunits in the enzyme molecule accompanied by rotation of the γ-subunit are supposed to occur in concert. In each of the states of the enzyme–substrate complex shown in Fig. 17a, one of the catalytic sites is always in the β_{TP} conformation, another in β_{DP}, and the third in β_E. We assume for definiteness that the closed catalytic site having the β_{TP} conformation initially contains ATP [state $\beta_{TP}(T)$]. This state is characterized by a high affinity for ATP. The second site, having the 'closed' β_{DP} conformation, contains ADP [state $\beta_{DP}(D)$]. The third catalytic site is free and has an 'open' conformation [state $\beta_E(-)$].

We consider how the electrostatic protein energy changes during the catalytic cycle of ATP hydrolysis in the case of a trisite scenario of enzyme operation (Fig. 17b). The first stage of the cycle is the entry of ATP into the empty catalytic center $\beta_E(-)$. It is known from biochemical data (see Section 3.2.2) that this stage is accompanied by a reduction in the free energy. Results of our calculations of $E_{\rm el}$ agree with this observation. They show that ATP binding to the enzyme in the $\beta_{TP}(T)\,\beta_{DP}(D)\,\beta_E(-)$ state is associated with a significant decrease in the system electrostatic energy [the transition $\beta_{TP}(T)\,\beta_{DP}(D)\,\beta_E(-) + ATP \rightarrow \beta_{TP}(T)\,\beta_{DP}(D)\,\beta_E(T)$]. As mentioned above, the energetically favorable ATP binding induces conformational rearrangement of the enzyme related to a change in the tilt angle of two large

domains of the β-subunit connected by a 'hinge' (see Fig. 7), which is in turn coupled to the turn of the γ-subunit.

A few scenarios of events initiated by ATP binding to the empty center $\beta_E(-)$ were considered in [127]. They differ in the stage of the catalytic cycle that immediately follows the binding [rotation of the γ-subunit or ATP hydrolysis in the $\beta_{TP}(T)$ center]. In one of the scenarios, part of the energy released during the ATP binding [the transition $\beta_{TP}(T)\beta_{DP}(D)\beta_E(-) + ATP \rightarrow \beta_{TP}(T)\beta_{DP}(D)\beta_E(T)$] is used to rotate the γ-subunit in the $\alpha_3\beta_3$ hexamer. According to Refs [31, 32], the bend in the β-subunit induces a stroke that causes it to rotate (Fig. 17b, transition from state 2 to state 3) and leads to corresponding conformational changes in the remaining subunits of the ATPase complex. Direct interaction between the β- and γ-subunits responsible for the energetic coupling in F_1-ATPase involves a conservative fragment of the β-subunit (β^{380}DELSEED^{386}). As shown in Fig. 17b, the structural transition from state 2 to state 3 is accompanied by an increase in the electrostatic constituent of the enzyme–substrate complex energy. It may be supposed that both transitions, 'state 1 → state 2' (energy-donating process) and 'state 2 → state 3' (energy-accepting process), occur cooperatively. This means that the energy released in the former process does not totally dissipate to heat; part of it is used to maintain the latter process. The design of the system ensures cooperative structural rearrangement of its subunits: the force generated by the bending of the $\beta_E(T)$ subunit causes the γ-subunit to rotate and thereby alters the state of other catalytic sites. In other words, ATP binding by the vacant catalytic site $\beta_E(-)$ results in conformational changes in all the three catalytic sites [the transition $\beta_{TP}(T)\,\beta_{DP}(D)\,\beta_E(T) \rightarrow \beta_{DP}(T)\,\beta_E(D)\,\beta_{TP}(T)$].

The next stage of the catalytic cycle is ATP hydrolysis or the $\beta_{DP}(T)\,\beta_E(D)\,\beta_{TP}(T) \rightarrow \beta_{DP}(D,P)\,\beta_E(D)\,\beta_{TP}(T)$ transition (from state 3 to state 4). The ATP hydrolysis reaction includes a stage at which an intermediate (a pentahedral complex) is produced as a result of the nucleophilic attack of the third phosphate of ATP (γ-phosphate) by a water molecule located inside the catalytic site in the immediate vicinity of ATP (see Fig. 6). It is believed that the water molecule involved in ATP hydrolysis is activated by the nearby deprotonated carboxylic group of Glu188 (55). The breakdown of the bond between ADP and γ-phosphate is accompanied by proton dissociation:

$$ADP{-}PO_3^{2-} + HOH \rightarrow ADP + HPO_4^{2-} + H^+ .$$

Two possible scenarios for the fate of the dissociated proton are considered: (a) its transfer to the carboxyl group of Glu188 (Fig. 17b, transition to the energy level 4a) with subsequent dissociation into the bulk solution, (b) its dissociation into the solution with subsequent hydrolysis of ATP (Fig. 17b, transition to the energy level 4b). It follows from Fig. 17b that the difference between the energy levels 4a and 4b is not very large compared with the energy gain from ATP binding.

As mentioned above, the ATP hydrolysis/synthesis reaction at catalytic sites of F_1-ATPase is reversible and has an equilibrium constant close to unity [36], meaning that the standard free energy for the reaction of $ATP + H_2O \rightleftarrows ADP + P_i$ proceeding in the active center of the enzyme is almost zero. This inference is questioned by Weber and Senior (see reviews [91–93]), who believe that the ATP/ADP ratio at the 'closed' catalytic site must depend on the process direction. The equilibrium is shifted toward the ATP production under conditions of ATP synthesis and toward the formation of ADP and P_i during ATP hydrolysis. Our calculations show that ATP hydrolysis at the 'closed catalytic site' of β_l is accompanied by a slight increase in the electrostatic constituent of the enzyme–substrate complex energy. We emphasize that the increase in the energy associated with ATP hydrolysis ($\Delta E_{ATP \rightarrow ADP+P_i}$) is significantly smaller than the energy gain from ATP binding. We note that under a different scenario of events initiated by ATP binding and in the case of electrostatic interactions taking the contribution of water molecules inside the protein globule into account, the ATP hydrolysis may occur practically without energy consumption (see Refs [127, 128] for the details).

An important conclusion following from the analysis of the energy diagram in Fig. 17b is that during the ATP synthesis at the catalytic site of $\beta_{DP}(T)$ (reaction $ADP + P_i \rightarrow ATP + H_2O$), the electrostatic constituent of the enzyme–substrate complex energy decreases rather than increases. This observation is consistent with the known standpoint that ATP synthesis inside the catalytic center occurs practically without energy consumption [36].

The further course of events after the ATP hydrolysis includes dissociation of the reaction products (P_i and ADP). Calculations in the framework of the electrostatic model [127, 128] indicate that dissociation of phosphate P_i (transition from state 4 to state 5) is accompanied by a reduction in the electrostatic interaction energy in the enzyme–substrate complex (Fig. 17b) in agreement with biochemical data, suggesting a relatively low affinity of P_i for F_1-ATPase [36, 64–68, 91–93].

On the other hand, dissociation of ADP (transition from state 5 to state 6) is accompanied by an appreciable increase in the electrostatic constituent of the enzyme complex energy, which hampers dissociation. At the same time, the increase in energy during the ADP dissociation in the presence of excess ATP in the solution surrounding the enzyme is compensated by the energetically favorable process of ATP binding to the emptied catalytic site (transition from state 6 to state 7). Thus, the complete catalytic cycle of ATPase accompanied by its structural rearrangement and the directional turn of the γ-subunit through 120° results in the disappearance of one ATP molecule in the solution surrounding the enzyme and the appearance of ADP and P_i. ATP hydrolysis in the aqueous medium is characterized by a decrease in the free energy; therefore, the F_1-ATPase energy of the entire system (enzyme, substrates, and reaction products dissolved in the medium) decreases after each turn of the rotor.

The above example shows that estimated changes in the electrostatic constituent of the enzyme–substrate complex energy in the framework of a relatively simple model are consistent with the known experimental data on the interaction of the substrates and reaction products with F_1-ATPase. Unfortunately, X-ray studies of the structure of F_1-ATPase do not provide reliable data on conformation of the enzyme–substrate complex at intermediate stages of the catalytic cycle. Nevertheless, its description by the above model proved useful for the analysis of F_1-ATPase work. The model can be extended by including intermediate states of the enzyme–substrate complex. Information about these states can be obtained by calculations using advanced methods of molecular dynamics and quantum chemistry. Results of calculations by these methods [111–114] confirm the important contribution of electrostatic interactions to the energetics of the catalytic cycle.

5.3 Stochastic–dynamic model of F_1-ATPase

5.3.1 Simulation of ATP hydrolysis by the isolated F_1-ATPase. In this section, we consider a mathematical model in which the dynamic equations for F_1-ATPase rotor rotation are described by phenomenological one-dimensional potentials [129, 130]. These potentials reflect conformational changes in the β-subunits throughout the catalytic cycle of ATP hydrolysis. A rotor whose position is specified by a coordinate θ is identified with a point mass moving in the given potential. The same potentials can be used to describe the motor operation during ATP synthesis when the rotor rotates in the opposite direction under the action of an external force generated by the F_0 membrane complex.

The shape of the model potential $V(\theta)$ is shown in Fig. 18. It is a sum of several functions. The function $V_{\mathrm{ATP}}(\theta-\theta_i)$ is the potential characterizing ATP binding by a catalytic site, θ is the rotor rotation angle, and $\theta_i = 90°$, 210°, and 330° are the values of θ corresponding to the three quasi-equilibrium positions of the rotor. The form of $V_{\mathrm{ATP}}(\theta-\theta_i)$ reflects the fact that the ATP binding is an energetically favorable process; in the absence of ATP, the potential for rotor rotation is unrelated to the θ angle. The potential $V_{\mathrm{ADP+P_i}}(\theta-\theta_i)$ corresponds to the presence of reaction products, ADP and P_i, in the active center. The close position of these two negatively charged molecules is energetically unfavorable and leads to a conformational change of the catalytic subunit that enables one of the reaction products to leave the active center. After dissociation of P_i, the function $V_{\mathrm{ADP+P_i}}(\theta-\theta_i)$ turns into the function $V_{\mathrm{ADP}}(\theta-\theta_i)$. The horizontal part of $V_{\mathrm{ADP}}(\theta-\theta_i)$ corresponds to the conformation of the β_{DP}(D)-catalytic subunit.

The potential depths are found from estimates of the energy of electrostatic interaction between the charged groups of an F_1-ATPase molecule and all reactants present in the active centers of the enzyme (see the preceding section). The depth of the V_{ATP} potential is $15\,k_{\mathrm{B}}T$ and the height of $V_{\mathrm{ADP+P_i}}$ is $10\,k_{\mathrm{B}}T$. The depth of the V_{ADP} potential well is assumed to be $5\,k_{\mathrm{B}}T$. The overall change in the energy during a single cycle of ATP hydrolysis is $20\,k_{\mathrm{B}}T$, which corresponds to the change in the free energy during hydrolysis of one ATP molecule under physiological conditions [49]. The 'reactivity' function $R(\theta-\theta_i)$ reflects the fact that the ATP synthesis/hydrolysis reactions occur only at a closed catalytic site. The function $S(\theta-\theta_i)$ phenomenologically describes steric hindrance restricting the access of reagents to the closed reaction center.

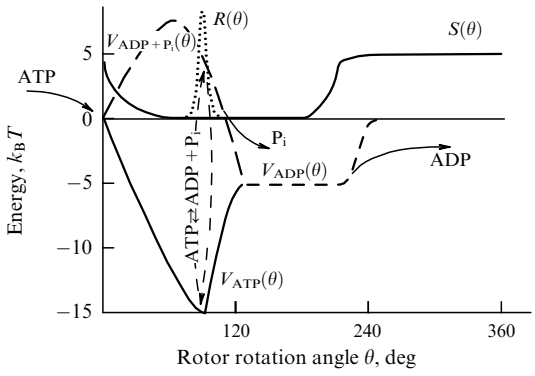

Figure 18. Model potential profiles for catalytic sites of F_1-ATPase containing ATP, ADP, or ADP + P_i depending on the rotor rotation angle θ. The model functions $R(\theta)$ and $S(\theta)$ respectively characterize specific features of ATP synthesis/hydrolysis reactions in catalytic centers and steric restrictions determining the accessibility of catalytic sites for reactants (based on [129, 130]).

To define the shape of the potential uniquely, we must take account of the filling of catalytic sites with substrates and reaction products. Then the potential becomes

$$V(\theta-\theta_i) = \bar{\psi}_{\mathrm{ATP}}\,V_{\mathrm{ATP}}(\theta-\theta_i) + \bar{\psi}_{\mathrm{ADP+P_i}}\,V_{\mathrm{ADP+P_i}}(\theta-\theta_i) + \bar{\psi}_{\mathrm{ADP}}\,V_{\mathrm{ADP}}(\theta-\theta_i)\,, \tag{15}$$

where the functions $\bar{\psi}_{\mathrm{ATP}}$, $\bar{\psi}_{\mathrm{ADP}}$, and $\bar{\psi}_{\mathrm{ADP+P_i}}$ signal the presence or absence of one substrate or another at the catalytic site (see [130] for the details). The resultant potential V_{s} is the sum of potentials for each of the three catalytic subunits:

$$V_{\mathrm{s}}(\theta) = V(\theta-\theta_1) + V(\theta-\theta_2) + V(\theta-\theta_3)\,. \tag{16}$$

The equation describing rotor rotation in the field of the potential V_{s} has the form

$$J\frac{\mathrm{d}^2\theta}{\mathrm{d}t^2} + \xi\frac{\mathrm{d}\theta}{\mathrm{d}t} = -\frac{\partial V_{\mathrm{s}}(\theta)}{\partial\theta} + f_{\mathrm{l}}(t)\,, \tag{17}$$

where J is the moment of inertia of the rotor, θ is the rotor rotation angle, ξ is the drag coefficient, and $f_{\mathrm{l}}(t)$ is the rotor torque due to thermal fluctuations. Characteristic frequencies of γ-subunit rotation are in the range of tens of hertz. Because of the high viscosity of the medium where the loaded rotor rotates ($\eta \approx 10^{-3}$ N cm^{-2} and $\xi \approx 10^{-21}$ N m s), the contribution of the inertial term $J\,\mathrm{d}^2\theta/\mathrm{d}t^2$ in Eqn (17) can be neglected. The equation must be supplemented by a system of kinetic equations describing stochastic processes of substrate entry and transformation at catalytic sites and the release of reaction products (see Ref. [130] for the details).

Figure 19a exemplifies calculations describing directions of rotor rotation at different ATP concentrations. Two extreme rotation regimes can be distinguished depending on the ATP concentration: (a) the prevalence of pauses related to waiting for the ATP entry (at low ATP concentrations) and (b) the prevalence of pauses produced by waiting for the ADP release (at high ATP levels). In both cases, the length of the pauses is roughly equal at intermediate ATP concentrations.

Figure 19b shows the ATP level dependence of the mean rotor rotation rate of the F_1 mechanochemical motor at different external loads on the rotor. Evidently, the directional rotor rotation rate increases to the maximum possible value as the ATP concentration increases to 1–2 mM or higher. It significantly decreases as the drag coefficient ξ increases. Figure 20 shows the dependences of the directional rotor rotation rate on the actin filament length attached to the rotor calculated for different ATP levels.[5] The theoretical curves in Figs 19 and 20 are in excellent quantitative agreement with the known experimental data [80]; this confirms the validity of the model.

5.3.2. Simulation of ATP synthesis by isolated F_1-ATPase under the action of an external force. In this section, we briefly summarize the results of the simulation of ATP synthesis by isolated F_1-ATPase that was observed in experiments on the rotation of the 'magnetic handle'

[5] Results shown in Figs 19 and 20 were obtained jointly with A F Pogrebnaya (see Refs [129–132] for the details).

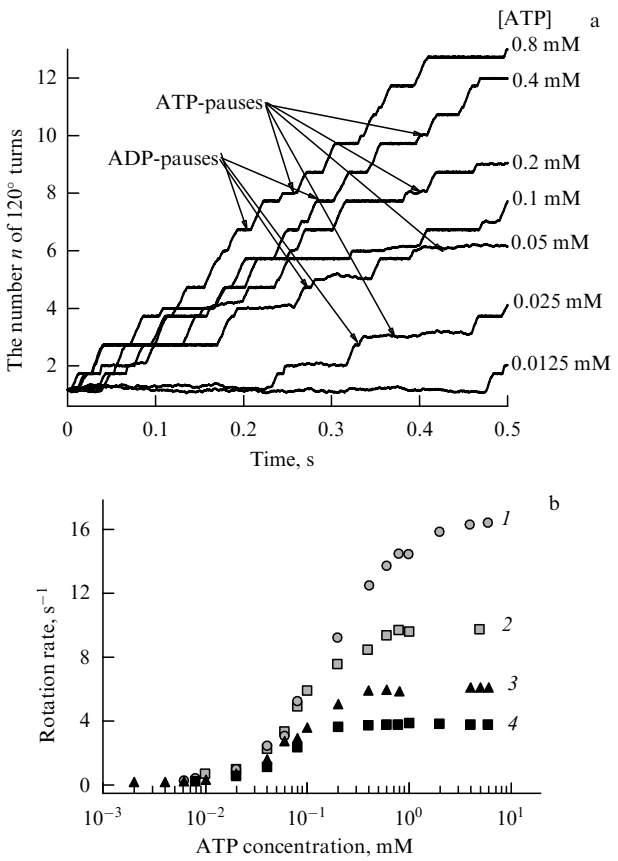

Figure 19. (a) Results of simulation of F_1-ATPase rotor rotations at different ATP concentrations. Drag coefficient $\xi = 3 \times 10^{-21}$ [N m s]. (b) The ATP level dependence of the mean rotor rotation rate at different rotor loads to which the following drag coefficients ξ correspond: *1* — 0.3×10^{-21} [N m s]; *2* — 0.5×10^{-21} [N m s]; *3* — 10^{-21} [N m s]; *4* — 2×10^{-21} [N m s] (based on [129, 130]).

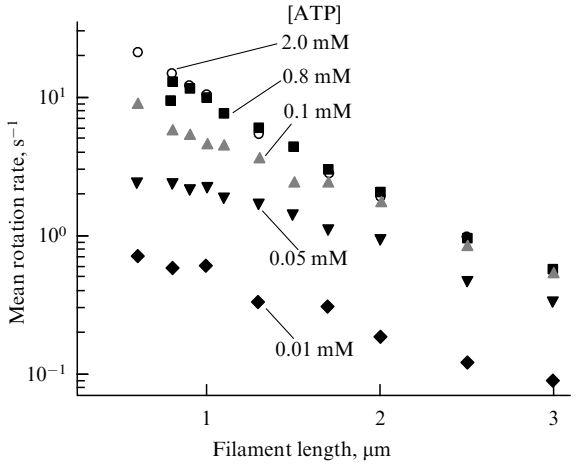

Figure 20. The dependence of the mean F_1-ATPase rotor rotation rate on the ATP concentration and the length L of the filament attached to the rotor (based on calculations in Ref. [131]). The drag coefficient ξ was calculated using formula (4).

attached to the γ-subunit [95]. Rotation of the γ-subunit by an external force causes periodic changes in the state of catalytic sites and thereby creates conditions for ATP synthesis or hydrolysis, depending on the direction of rotor rotation. It is supposed that ATP synthesis and hydrolysis are associated with identical conformational changes that occur in the opposite order, however. The entry of ADP and P_i, and the synthesis and dissociation of ATP are regarded as random events. The model has allowed describing ATP synthesis without the introduction of an additional assumption into the system of equations and model potentials considered in the preceding sections.

The results of simulations of forced rotor rotation at different ATP concentrations indicate that the rotation rate increases as the angular momentum of the external force increases, regardless of the ATP level [131, 132]. The rotation dynamics depend on model parameters (the external force F_{ext}, the ADP concentration, and the drag coefficient ξ) that determine characteristic times in the system. At small F_{ext}, the rotor rotates in a manifestly stepwise manner with pauses caused by waiting for the ADP entry into a catalytic center; the duration of the pauses decreases with increasing the ATP concentration. At sufficiently high F_{ext} values, the 120° turns occur in the absence of ATP synthesis, while the operating efficiency of the enzyme decreases.

5.4 The 'trigger' model of F_1-ATPase

In this section, we present a phenomenological mathematical model describing the trigger regime of energy-dependent conformational transitions of β-subunits ('open' conformation ↔ 'closed' conformation) [133, 134]. The main purpose of this model is to analyze the effect of elastic strains of β-subunits described in [31, 70].

In the presence of excess ATP in the medium, F_1-ATPase operates without the failure possible in the case of diffusional restrictions: the next ATP molecule enters the open 'pocket' of a catalytic site as soon as it is emptied. At a low ATP level, occasional delays in the ATP entry into the pocket of an empty catalytic site must be taken into consideration. We assume that the ATP concentration in the medium is high, and neglect the fluctuational character of the dynamics of the β- and γ-subunits in the first approximation.

The sought variables in the trigger model are the angle β_i [the opening angle of a β_i-subunit or the angle between two large domains of this subunit (Fig. 6a)] and the elastic force moment τ_i ($i = 1, 2, 3$ labels the β-subunits). The system of equations for the change in β_i from $\pi/6$ to 0 characterizing the closure of the 'pocket' of the catalytic site has the form

$$\zeta \frac{d\beta_i}{dt} = M(\beta_i) - \tau_i , \tag{18}$$

$$\mu \frac{d\tau_i}{dt} = kl^2\beta_i - \tau_i - \tau_0 , \tag{19}$$

where $M(\beta_i)$ is the N-shaped moment of forces arising upon the ATP binding by the catalytic site of β_i (the amplitude of this moment is $A \approx 40$ pN nm), τ_i is the elastic force moment arising upon deformation of the β_i-subunit, $\mu \approx 1-2$ ms is the characteristic time of bond cleavage during hydrolysis ($ATP \rightarrow ADP + P_i$) at the catalytic site, $k = 4$ pN nm^{-1} is the stiffness factor of the construction, $l \approx 3$ nm is the elastic force moment arm, and $\zeta \sim 10^{-21}$ N m s is the drag coefficient determined by the Stokes drag of a filament or a bead attached to the rotor (in a model for immobilized F_1-ATPase operating under mechanical load). It is believed that the DELSEED segment of the closing β-subunit makes contact with the γ-subunit and 'turns' the rotor. A change in β by $\pi/6$ corresponds to a turn of the rotor through the angle $2\pi/3$. Because the moment of inertia and the Stokes drag of the subunits themselves are small, they can be neglected. The

parameter $\tau_0 \approx 20$ pN nm is determined by the residual elastic stress of the β-subunit.

The storage of the elastic strain energy is delayed with respect to evolution of the β angle characterizing the tilt of the two large domains of the β-subunit connected by a hinge (see Fig. 7). The dynamics of this process are described in the first approximation by Eqn (19) for τ_i. It is assumed, for simplicity, that the 'closing' moment $M(\beta_i)$ at $0 < \beta_i < \pi/6$ depends on β_i and τ_i linearly. The angle β_i opens from 0 to $\pi/6$ under the effect of $M_1(\beta_i)$. Then

$$\varepsilon \frac{\mathrm{d}\beta_i}{\mathrm{d}t} = M_1(\beta_i) \approx -\alpha M(\beta_{i-1}) + \tau_i \,, \tag{20}$$

where $M(\beta_{i-1})$ is the moment created by the closing β_{i-1}-subunit ($\alpha < 1$); $\varepsilon \ll \zeta$ because the resistance to friction or the drag coefficient ε is very small when the angle β_i opens (enlarges).

As shown in Refs [133, 134], Eqns (18)–(20) have periodic solutions at a high concentration of ATP in the medium. The starting conditions at each step are chosen such that the initial deviation of β_i exceeds a certain small threshold value. The analysis of numerical solutions showed that the time during which β_i changes by $\pi/6$ and, accordingly, the rotor rotation angle θ changes by $2\pi/3$ is of the order of $\zeta/A \ll \mu$ [here, A is the amplitude of the moment $M(\beta_i)$], in agreement with experiment (Fig. 20c). Therefore, the total time T of rotor rotation by 2π largely depends on the time of macroergic bond cleavage:

$$T \approx 3\mu + 3\,\frac{\zeta}{A} \,. \tag{21}$$

The period increases with the moment of forces from an external load applied to the rotor. Taking a more complicated function $M(\beta_i)$ allows simulating the two-step change of β during hydrolysis [133, 134].

To conclude this section, we emphasize that the theory of F_0F_1 ATP synthase is far from complete. Listed below are only a few unresolved problems that might be interesting for physicists.

(1) How can the noises of different natures be adequately taken into account in the dynamics of F_0F_1 ATP synthase-like molecular machines? This question implies an analysis of the contribution of thermal and shot noises related to the nonuniformity of the diffusionally controlled ATP and ADP entry into the catalytic centers of the enzyme and noises due to the scatter of the times of macroergic bond cleavage during ATP hydrolysis (analog of flicker noises).

(2) How can the 'elasticity' of elements of a macromolecular construction be calculated in the case of deformation of different subunits (α, β, and γ)?

(3) How can the notions developed in theoretical studies on the Brownian motion of particles in complicated potential landscapes (receiving energy from an external source [135]) be applied to the calculation of the F_0F_1 ATP synthase rotor rotation?

The discussion of one more problem of theoretical biophysics is in order in connection with the aforesaid. There are a few scientific schools in this country that have for many years been engaged in research on autowave processes in biological membranes (in Nizhny Novgorod [136], in Pushchino [137, 138], at Moscow State University [139], etc.). The state of research in this field abroad is comprehensively described in the fundamental monograph by J Murray (a Russian translation of its volume 1 was published in 2009 [140]). All the authors in one way or another use nonlinear characteristics of the membrane channel conductance that are frequently fixed based on general considerations reliant on experimental findings. We believe that new data on the structural and functional organization of membrane ATPases will help elucidate concrete relations between the theory of ion channel conductivity and nonlinear processes considered by different authors in describing biomembranes. Finally, Ref. [141] is worthy of special mention because it concerns the continuity of the ATP synthase theory and the theory of bacterial flagellar motor.

6. Concluding remarks

In this review, we considered modern concepts of the physicochemical mechanism of the action of proton ATP synthase, a principal macromolecular device catalyzing formation of ATP molecules — the main energy 'currency' of the living cell. The ATP synthase complex embedded in the plasma membrane operates as an energy-converting macromolecular machine driven by the transmembrane electrochemical potential difference of hydrogen ions ($\Delta\mu_{H^+}$). The electric current passing through the membrane via the F_0 complex (with protons playing the role of current carriers) governs rotation of the rotor (intramembranous c_n ring). The c_n ring of the molecular 'electric motor' is connected to the rotor of the F_1 mechanochemical motor (γ-subunit), whose rotation ensures the ATP synthesis from ADP and P_i. F_0F_1 ATP synthase is a reversible molecular machine capable of synthesizing and hydrolyzing ATP. When the rotor of the F_1 motor rotates against the F_0 rotor (driven by the energy of hydrolyzed ATP molecules), F_0F_1 ATP synthase functions as a proton pump generating $\Delta\mu_{H^+}$. There is direct experimental evidence that the rotors of both F_0F_1 ATP synthase motors (F_0 and F_1) actually rotate during the work of this macromolecular device.

F_0F_1 ATP synthase is a macromolecular machine remarkable for its highly efficient energy conversion ($\eta \approx 90-100\%$). The high efficiency of F_0F_1 ATP synthase is due to its peculiar design accounting for the tight coupling between chemical and mechanical stages of the catalytic cycle, which reduces the energy dissipation to heat to a minimum. It may be said that F_0F_1 ATP synthase is an 'enthalpic' molecular machine [1–3] characterized by insignificant changes in the entropy ($\Delta S \approx 0$). This means that F_0F_1 ATP synthases work as molecular motors, although they cannot be viewed as thermal machines in the ordinary sense. These molecular motors, unlike macroscopic thermal machines, do not need to be equipped with special devices, such as 'refrigerators' or 'heaters.'

Proton ATP synthase, with the characteristic size ≈ 10 nm, is the smallest of the known natural rotating motors. At the same time, it seems to be the most 'powerful' mechanochemical molecular motor using ATP molecules as a chemical 'fuel.' The torque created by a single F_1-ATPase molecule (F_1 motor) is $N \approx 40-45$ pN nm (it develops the force $F \approx 40-45$ pN). The mean rotor rotation rate amounts to 300 rpm.

We have considered the work of F_0F_1 ATP synthase, which is only one, albeit very important, molecular machine of the living cell. Hundreds of billions of such molecular machines operate in each living organism to maintain reproduction of a 'chemical fuel' in the form of ATP

Table 1. Comparative characteristics of molecular motors (from Ref. [142]).

Motor/pathway	Motion step	Max. force	Max. efficiency	Mode of motion
α-, β-, and γ-subunits of F_1	Turn by 120°	40 pN	≈ 100%	Rotation
Myosin/Actin	Alternating	3–5 pN	≈ 20%	Steps, jumps
Kinesin/Microtube	8 nm shift	5 pN	≈ 50%	Steps
RNA polymerase/DNA	0.34 nm shift	14 pN	≈ 20%	'Crawling'

molecules. It is opportune to mention that over 50 kg of ATP molecules are synthesized daily in the body of an adult person, and are utilized during the same time to perform different forms of work (chemical, osmotic, and mechanical).

Table 1 compares characteristics of different molecular motors, including the so-called 'linear' ones (myosin, kinesin) moving along 'guideways' (actin filaments and tubulin microtubes) to maintain contractile and transport activities of isolated cells and whole organisms and RNA polymerase traveling along the DNA strand. It can be seen that the maximum force generated by the rotor of the F_1 mechano-chemical motor is much greater than that developed by 'linear' motors. Evidently, rotation is a more efficient and cost-effective mode of operation than the translational motion of 'linear' biological motors.

The bacterial electric motor rotating a long helical flagellum is a much more sophisticated device than F_0F_1-ATP synthase [32]. This motor is driven by the electrochemical potential of hydrogen or sodium ions. Its stator and rotor are made of tens of proteins, including the so-called motor proteins A and B arranged in a circle. The joint operation of many such molecules creates a strong torque ($N \approx$ 4000 pN nm). Flagellar electric motors are high-speed ($\sim 400-1700$ rps) devices, even if they have to rotate long flagellae (~ 10 μm). Over 1000 protons pass through a motor during one revolution of its rotor. The efficiency of bacterial motors is very high. Bacteria can swim at the average translational speed 25 μm s^{-1}, which amounts to more than 100 μm s^{-1} for certain species. In other words, a bacterium travels ten times its own length in one second.

The variety of molecular motors that came into being over three billion years ago is not limited to the above examples. Experimental and theoretical studies of natural nanosized motors continue. Modern physical methods are of primary importance for the investigation of biophysical mechanisms of action of biological machines; they are used not only to observe the behavior of individual protein molecules and protein complexes but also to purposefully manipulate individual macromolecules.

This work was supported by the RFBR (project 09-04-00978). The authors are grateful to A F Pogrebnaya and A V Kargovsky for their invaluable contribution to the construction and numerical realization of the mathematical models described in Sections 5.2–5.4 and to M K Aliev and I G Minkevich for critically reading the manuscript. Thanks are also due to W Ebeling, L Schimansky-Gaier, and A Lavrova of Humboldt-Universität, Berlin, for the enlightening discussions on theoretical problems of molecular motors.

References

1. Blumenfeld L A *Problemy Biologicheskoi Fiziki* (Problems of Biological Physics) (Moscow: Nauka, 1974) [Translated into English (Heidelberg: Springer-Verlag, 1981)]
2. Blumenfeld L A, Tikhonov A N *Biophysical Thermodynamics of Intracellular Processes: Molecular Machines of the Living Cell* (New-York: Springer-Verlag, 1994)
3. Chernavskii D S, Chernavskaya N M *Belok-Mashina: Biologicheskie Makromolekulyarnye Konstruktsii* (Protein Machine. Biological Macromolecular Constructions) (Moscow: Yanus-K, 1999)
4. Chernavskii D S, Khurgin Yu I, Shnol' S E *Mol. Biol.* **1** 419 (1967)
5. Romanovsky Yu M, Ebeling W (Eds) *Molekulyarnaya Dinamika Fermentov* (Molecular Dynamics of Enzymes) (Moscow: Izd. Moskovskogo Universiteta, 2000)
6. Rubin A B *Biofizika* (Biophysics) Vol. 1 (Moscow: Izd. Moskovskogo Universiteta, 2004)
7. Asbury C L *Curr. Opin. Cell Biol.* **17** 89 (2005)
8. Carter N J, Cross R A *Curr. Opin. Cell Biol.* **18** 61 (2006)
9. Westermann S, Drubin D G, Barnes G *Annu. Rev. Biochem.* **76** 563 (2007)
10. Borgia A, Williams P M, Clarke J *Annu. Rev. Biochem.* **77** 101 (2008)
11. Marshall R A et al. *Annu. Rev. Biochem.* **77** 177 (2008)
12. Joo Ch et al. *Annu. Rev. Biochem.* **77** 51 (2008)
13. Herbert K M, Greenleaf W J, Block S M *Annu. Rev. Biochem.* **77** 149 (2008)
14. Hamdan S M, Richardson C C *Annu. Rev. Biochem.* **78** 205 (2009)
15. Gennerich A, Vale R D *Curr. Opin. Cell Biol.* **21** 59 (2009)
16. Moffitt J R et al. *Annu. Rev. Biochem.* **77** 205 (2008)
17. Block S M, Goldstein L S, Schnapp B J *Nature* **348** 348 (1990)
18. Svoboda K et al. *Nature* **365** 721 (1993)
19. Finer J T, Simmons R M, Spudich J A *Nature* **368** 113 (1994)
20. Vale R D *Cell* **112** 467 (2003)
21. Howard J, Hudspeth A J, Vale R D *Nature* **342** 154 (1989)
22. Rice S et al. *Nature* **402** 778 (1999)
23. Yildiz A et al. *Science* **303** 676 (2004)
24. Kon T et al. *Nature Struct. Mol. Biol.* **12** 513 (2005)
25. Grishchuk E L et al. *Nature* **438** 384 (2005)
26. McIntosh J et al. *Cell* **135** 322 (2008)
27. Block S M *Biophys. J.* **92** 2986 (2007)
28. Shiroguchi K, Kinosita K (Jr.) *Science* **316** 1208 (2007)
29. Ebeling W, Schimansky-Gaier L, Romanovsky Yu M *Stochastic Dynamics of Reacting Biomolecules* (River Edgee, N.J.: World Scientific, 2002)
30. Shaitan K V, in *Stochastic Dynamics of Reacting Biomolecules* (River Edgee, N.J.: World Scientific, 2002) p. 285
31. Oster G, Wang H *Biochim. Biophys. Acta* (*BBA*) — *Bioenergetics* **1458** 482 (2000)
32. Oster G, Wang H *Trends Cell Biol.* **13** 114 (2003)
33. Keller D, Bustamante C *Biophys. J.* **78** 541 (2000)
34. Bustamante C, Keller D, Oster G *Acc. Chem. Res.* **34** 412 (2001)
35. Xing J et al. *Proc. Natl. Acad. Sci. USA* **103** 1260 (2006)
36. Boyer P D *Biochim. Biophys. Acta* (*BBA*) — *Bioenergetics* **1140** 215 (1993)
37. Boyer P D *Annu. Rev. Biochem.* **66** 717 (1997)
38. Junge W, Lill H, Engelbrecht S *Trends Biochem. Sci.* **22** 420 (1997)
39. Stock D et al. *Curr. Opin. Struct. Biol.* **10** 672 (2000)
40. Walker J (Guest Ed.) *Biochim. Biophys. Acta* **1458** (2–3) (2000), Special Issue
41. *J. Bioenerg. Biomembr.* **32** (4–5) (2000), Minireview Series, ATP Synthesis in the Year 2000: Current Views about Structure, Motor Components, Energy Interconversions and Catalytic Mechanisms, Pt. 1, 2
42. Harvey W R, Boutilier R G, Nelson N (Eds) *J. Exp. Biol.* **203** (1) (2000), Special issue
43. Capaldi R A, Aggeler R *Trends Biochem. Sci.* **27** 154 (2002)
44. Von Ballmoos C, Wiedenmann A, Dimroth P *Annu. Rev. Biochem.* **78** 649 (2009)
45. Von Ballmoos C, Cook G M, Dimroth P *Annu. Rev. Biophys.* **37** 43 (2008)

46. Mitchell P *Theor. Exp. Biophys.* **2** 159 (1969)
47. Skulachev V P *Membrane Bioenergetics* (New York: Springer-Verlag, 1988)
48. Nicholls D G, Ferguson S J *Bioenergetics 3* (San Diego, Calif.: Academic Press, 2002)
49. Nelson D L, Cox M M *Lehninger Principles of Biochemistry* 4th ed. (New York: W.H. Freeman, 2005)
50. Alberty R A *J. Biol. Chem.* **244** 3290 (1969)
51. Gräber P *Curr. Topics Membr. Transp.* **16** 215 (1982)
52. Kramer D M, Sacksteder C A, Cruz J A *Photosynth. Res.* **60** 151 (1999)
53. Trubitsin B V, Tikhonov A N *J. Magn. Res.* **163** 257 (2003)
54. Tikhonov A N et al. *Biochim. Biophys. Acta* **1777** 285 (2008)
55. Abrahams J P et al. *Nature* **370** 621 (1994)
56. Leslie A G W, Walker J E *Philos. Trans. R. Soc. Lond. B* **355** 465 (2000)
57. Groth G, Pohl E *J. Biol. Chem.* **276** 1345 (2001)
58. Seelert H et al. *Nature* **405** 418 (2000)
59. Stock D, Leslie A G W, Walker J E *Science* **286** 1700 (1999)
60. Menz R I, Walker J E, Leslie A G *Cell* **106** 331 (2001)
61. Kabaleeswaran V et al. *EMBO J.* **25** 5433 (2006)
62. Oster G, Wang H, in *Encyclopedia of Molecular Biology* (Ed. T Creighton) (New York: Wiley, 1999) p. 211
63. Shirakihara Y et al. *Structure* **5** 825 (1997)
64. Grubmeyer C, Cross R L, Penefsky H S *J. Biol. Chem.* **257** 12092 (1982)
65. Cunningham D, Cross R L *J. Biol. Chem.* **263** 18850 (1988)
66. Senior A E *J. Bioenerg. Biomem.* **24** 479 (1992)
67. Milgrom Y M, Murataliev M B, Boyer P D *Biochem. J.* **330** 1037 (1998)
68. Penefsky H S, Cross R L *Adv. Enzymol. Relat. Areas Mol. Biol.* **64** 173 (1991)
69. Antes D et al. *Biophys. J.* **85** 695 (2003)
70. Sun S et al. *Eur. Biophys. J.* **32** 676 (2003)
71. Vinogradov A D *J. Exp. Biol.* **203** 41 (2000)
72. Duncan T M et al. *Proc. Natl. Acad. Sci. USA* **92** 10964 (1995)
73. Zhou Y et al. *Biochim. Biophys. Acta* (*BBA*) — *Bioenergetics* **1275** 96 (1996)
74. Zhou Y, Duncan T M, Cross R L *Proc. Natl. Acad. Sci. USA* **94** 10583 (1997)
75. Sabbert D, Engelbrecht S, Junge W *Nature* **381** 623 (1996)
76. Sabbert D, Engelbrecht S, Junge W *Proc. Natl. Acad. Sci. USA* **94** 4401 (1997)
77. Häsler K, Engelbrecht S, Junge W *FEBS Lett.* **426** 301 (1998)
78. Noji H et al. *Nature* **386** 299 (1997)
79. Yasuda R et al. *Cell* **93** 1117 (1998)
80. Kinosita K et al. *Philos. Trans. R. Soc. Lond. B* **355** 473 (2000)
81. Sambongi Y et al. *Science* **286** 1722 (1999)
82. Tanabe M et al. *J. Biol. Chem.* **276** 15269 (2001)
83. Yasuda R et al. *Nature* **410** 898 (2001)
84. Shimabukuro K et al. *Proc. Natl. Acad. Sci. USA* **100** 14731 (2003)
85. Nishizaka T et al. *Nature Struct. Mol. Biol.* **11** 142 (2004)
86. Kinosita K, Adachi K, Itoh H *Annu. Rev. Biophys. Biomol. Struct.* **33** 245 (2004)
87. Ueno H et al. *Proc. Natl. Acad. Sci. USA* **102** 1333 (2005)
88. Sakaki N et al. *Biophys. J.* **88** 2047 (2005)
89. Adachi K et al. *Cell* **130** 309 (2007)
90. Boyer P D *FEBS Lett.* **512** 29 (2002)
91. Weber J, Senior A E *Biochim. Biophys. Acta* (*BBA*) — *Bioenergetics* **1319** 19 (1997)
92. Weber J, Senior A E *Biochim. Biophys. Acta* (*BBA*) — *Bioenergetics* **1458** 300 (2000)
93. Senior A, Nadanaciva S, Weber J *Biochim. Biophys. Acta* (*BBA*) — *Bioenergetics* **1553** 188 (2002)
94. Weber J, Senior A E *J. Biol. Chem.* **276** 35422 (2001)
95. Itoh H et al. *Nature* **427** 465 (2004)
96. Yasuda R et al. *Proc. Natl. Acad. Sci. USA* **100** 9314 (2003)
97. Diez M et al. *Nature Struct. Mol. Biol.* **11** 135 (2004)
98. Ma J et al. *Structure* **10** 921 (2002)
99. Furuike S et al. *Science* **319** 955 (2008)
100. Hossain M D et al. *Biophys. J.* **95** 4837 (2008)
101. Suzuki T et al. *J. Biol. Chem.* **277** 13281 (2002)
102. Elston T, Wang H, Oster G *Nature* **391** 510 (1998)
103. Wang H, Oster G *Nature* **396** 279 (1998)
104. Grabe M , Wang H, Oster G *Biophys. J.* **78** 2798 (2000)
105. Wang H, Oster G *Europhys. Lett.* **57** 134 (2002)
106. Jain S, Nath S *FEBS Lett.* **476** 113 (2000)
107. Sun S X, Wang H, Oster G *Biophys. J.* **86** 1373 (2004)
108. Dittrich M, Hayashi S, Schulten K *Biophys. J.* **85** 2253 (2003)
109. Böckmann R A, Grubmüller H *Nature Struct. Biol.* **9** 198 (2002)
110. Böckmann R A , Grubmüller H *Biophys. J.* **85** 1482 (2003)
111. Yang W et al. *Proc. Natl. Acad. Sci. USA* **100** 874 (2003)
112. Strajbl M, Shurki A, Warshel A *Proc. Natl. Acad. Sci. USA* **100** 14834 (2003)
113. Gao Y Q et al. *Proc. Natl. Acad. Sci. USA* **100** 11339 (2003)
114. Romanovsky Yu M, Kargovskii A V, in *Nelineinye Volny 2008* (Nonlinear Waves 2008) (Eds A V Gaponov, V I Nekorkin) (N. Novgorod: IPF RAN, 2009) p. 223
115. Nartsissov Ya R, Mashkovtseva E V *Biofizika* **50** 1048 (2005) [*Biophysics* **50** 905 (2005)]
116. Nartsissov Y R, Mashkovtseva E V *J. Theor. Biol.* **242** 300 (2006)
117. Pänke O, Rumberg B *Biochim. Biophys. Acta* (*BBA*) — *Bioenergetics* **1412** 118 (1999)
118. Cherepanov D A, Mulkidjanian A Y, Junge W *FEBS Lett.* **449** 1 (1999)
119. Pänke O et al. *Biophys. J.* **81** 1220 (2001)
120. Rastogi V K, Girvin M V *Nature* **402** 263 (1999)
121. Fillingame R H et al. *Biochim. Biophys. Acta* (*BBA*) — *Bioenergetics* **1458** 387 (2000)
122. Fillingame R H, Angevine C M, Dmitriev O Y *Biochim. Biophys. Acta* (*BBA*) — *Bioenergetics* **1555** 29 (2002)
123. Fillingame R H, Dmitriev O Y *Biochim. Biophys. Acta* (*BBA*) — *Bioenergetics* **1565** 232 (2002)
124. Xing J, Wang H, Oster G *Biophys. J.* **89** 1551 (2005)
125. Xing J et al. *Biophys. J.* **87** 2148 (2004)
126. Xing J, Liao J-C, Oster G *Proc. Natl. Acad. Sci. USA* **102** 16539 (2005)
127. Tikhonov A N, Pogrebnaya A F, Romanovsky Yu M *Biofizika* **48** 1052 (2003) [*Biophysics* **48** 970 (2003)]
128. Pogrebnaya A F, Romanovsky Y M, Tikhonov A N *Proc. SPIE* **5068** 27 (2003)
129. Pogrebnaya A F, Romanovsky Y M, Tikhonov A N *Proc. SPIE* **5330** 120 (2004)
130. Pogrebnaya A, Romanovsky Y, Tikhonov A *Fluct. Noise Lett.* **5** L217 (2005)
131. Pogrebnaya A F, PhD Thesis (Moscow: Lomonosov Moscow State University. Biol. Department, 2005)
132. Pogrebnaya A F *Komp'yuternye Issledovaniya Modelirovanie* **1** 217 (2009)
133. Kargovsky A V, Romanovsky Yu M, Tikhonov A N *Biofizika* **54** 5 (2009) [*Biophysics* **54** 1 (2009)]
134. Kargovsky A V et al., in *Dinamicheskie Modeli Protsessov v Kletkakh i Subkletochnykh Nanostrukturakh* (Dynamic Models of Processes in Cells and Subcellular Nanostructures) (Eds G Yu Riznichenko, A B Rubin) (Moscow–Izhevsk: RKhD, 2009) p. 69
135. Fiasconaro A, Ebeling W, Gudowska-Nowak E *Eur. Phys. J. B* **65** 403 (2008)
136. Nekorkin V I *Usp. Fiz. Nauk* **178** 313 (2008) [*Phys. Usp.* **51** 295 (2008)]
137. Ivanitskii G R, Krinskii V I, Sel'kov E E *Matematicheskaya Biofizika Kletki* (Mathematical Biophysics of the Cell) (Moscow: Nauka, 1978)
138. Borisyuk G N et al. *Usp. Fiz. Nauk* **172** 1189 (2002) [*Phys. Usp.* **45** 1073 (2002)]
139. Plusnina T Yu et al. *J. Biol. Syst.* **16** 197 (2008)
140. Murray J D *Mathematical Biology I. An Introduction* (Berlin: Springer-Verlag, 2002) [Translated into Russian (Moscow–Izhevsk: RKhD. Inst. Komp'yut. Issled., 2009)]
141. Elston T C, Oster G *Biophys. J.* **73** 703 (1997)
142. Kinosita K (Jr.) et al. *Cell* **93** 21 (1998)